NASA Contractor Report 165683

DEVELOPMENT OF MBE GROWN Pb-SALT SEMICONDUCTOR LASERS FOR THE 8.0 TO 15.0 MICROMETER SPECTRAL REGION

Matthew D. Miller

Perkin-Elmer Corporation
100 Wooster Heights Road
Danbury, CT 06810

CONTRACT NAS1-14996
MARCH 1981

National Aeronautics and
Space Administration

Langley Research Center
Hampton, Virginia 23665

FINAL REPORT

DEVELOPMENT OF MBE GROWN Pb-SALT SEMICONDUCTOR LASERS FOR THE 8.0 TO 15.0 MICROMETER SPECTRAL REGION

Contract NAS1-14996

Submitted to

National Aeronautics and Space Administration
Langley Research Center
Hampton, Virginia 23665

Dr. James Hoell, Contract Manager

by

PERKIN-ELMER
100 Wooster Hgts. Rd.
Danbury, Connecticut 06810

Prin. Inves.: Dr. Matthew D. Miller

TABLE OF CONTENTS

1.0 Introduction and Summary

1.1 Program Objectives

The objective of this program was to develop a family of high performance tunable diode lasers suitable for use as local oscillators in a passive Laser Heterodyne Spectrometer (LHS). The diodes, based upon lead-tin telluride, were intended to operate in the 8-15um region, with specific target wavelengths of 893.37 cm^{-1} (11.2um) and 1081.1 cm^{-1} (9.25um). Specific goals included:

1) confirmation of technology viability by demonstrating laser operation, either pulsed or continuous wave

2) technology improvement to permit CW operation at 20°K with total output power of 50 microwatts

3) control of alloy composition to permit specification of wavelength at temperature

4) improvement in device reliability with regard to room temperature shelf life and degradation due to thermal cycling

5) delivery of lasers to NASA Langley Research Center for evaluation.

1.2 Approach

The approach was to utilize multiple source molecular beam epitaxy (MBE) to grow precisely controlled multilayer structures of (PbSn)Te on BaF_2 substrates and to fabricate diodes from the grown layers using standard integrated circuit processes (including photolithography, selective etching, and vacuum deposition of metals and insulators). This novel approach to laser fabrication required refinements in crystal growth and materials processing techniques and significant developments in device fabrication techniques. The program also included packaging refinements aimed at solving the thermal cycling problem and metallization changes aimed at the room temperature shelf life problem.

1.3 Summary of Results

Lasers were fabricated and delivered which operated cw from 10μm to 14μm, and for which cw operation was obtained at heat sink temperatures from 12°K to 60°K. Maximum multimode cw output power was 10-20 uw.

These lasers survived 1 month storage at 40°C and 1 year storage at room temperature. They also survived repetitive thermal cycling without degradation, thereby demonstrating that these two failure mechanisms are not fundamental, and that appropriate packaging and metallization can lead to reliable devices.

The shortfall in output power was initially ascribed to imperfect cavity formation due to the wet-chemical processes involved. However, ion-milled structures with excellent cavity cosmetics failed to improve output power significantly. We now believe that the low power of these lasers was due to the crystal lattice mismatch between (PbSn)Te and the BaF_2 substrates.

1.4 Recommendations

Multiple source molecular beam epitaxy has been shown to be a viable growth technology offering many advantages in flexibility and control compared to other crystal growth techniques. The selection of substrate is critical.

For the long range, substantial improvements can be anticipated from close-confined structures grown by MBE on lattice-matched bulk Pb-salt substrates. Electrical and optical confinement can be achieved either by composition variation (double heterostructure lasers) or by carrier concentration gradients introduced with extrinsic dopant control. Indeed, the wide tuning range and high temperature operation demonstrated during this program are proof of excellent confinement.

The thin-film processes developed in this program offer substantial cost reduction by providing the capability for mass production of standard devices. Photolithographic techniques coupled with the ease of MBE growth will permit fabrication of buried heterostructures, which have proven invaluable for mode control in the III-V semiconductor lasers.

2.1 General Description of Crystal Growth

The single crystal $(Pb_{1-x}Sn_x)Te$ films are grown by multiple source molecular beam epitaxy (MBE). This growth technique is a highly refined form of vacuum evaporation. A crystal is built up, one monolayer at a time, by the controlled deposition of its constituents on a heated substrate. If the substrate closely matches the crystal structure, lattice constant, and thermal expansion coefficient of the deposited film, orderly crystal growth results.

2.2 Perkin-Elmer Multiple Source MBE System

Figure 1 is a schematic drawing of Perkin-Elmer's "Research" MBE crystal grower, while figure 2 is a photograph showing the actual equipment. The growth chamber is to the left of the isolation valve, and the preparation and analysis chamber is to the right. Films are analyzed in-situ for crystallography by low energy electron diffraction (LEED) and for elemental surface composition by Auger spectroscopy. The gas valves and ion gun are for substrate cleaning, as required. For growth of the Pb-salts on BaF_2 substrates, heat cleaning prior to growth is sufficient. Source materials are evaporated from individually liquid-nitrogen shrouded graphite Knudsen cells. The cells are independently controlled, and are held isothermal to $\pm 1^{\circ}C$. Maximum cell temperature is about $1300^{\circ}C$. The quadrupole mass spectrometer monitors evaporant flux and residual gas in the growth chamber, whose base pressure is 10^{-10} torr.

Particular attention has been given to the Knudsen cell design to make the cells clean, isothermal, and reliable. The body is machined from a rod of spectroscopic grade graphite, and a graphite cover and collimating orifice are pressed into the top. Tungsten-in-alumina heater windings are driven by a proportional temperature controller and are wrapped with rippled Ta foil to hold them tightly in place and to reflect heat. The gold-plated copper liquid-nitrogen-cooled shroud reflects additional heat and also condenses outgassing contaminants. The cell temperature is measured by a W/Re thermocouple embedded

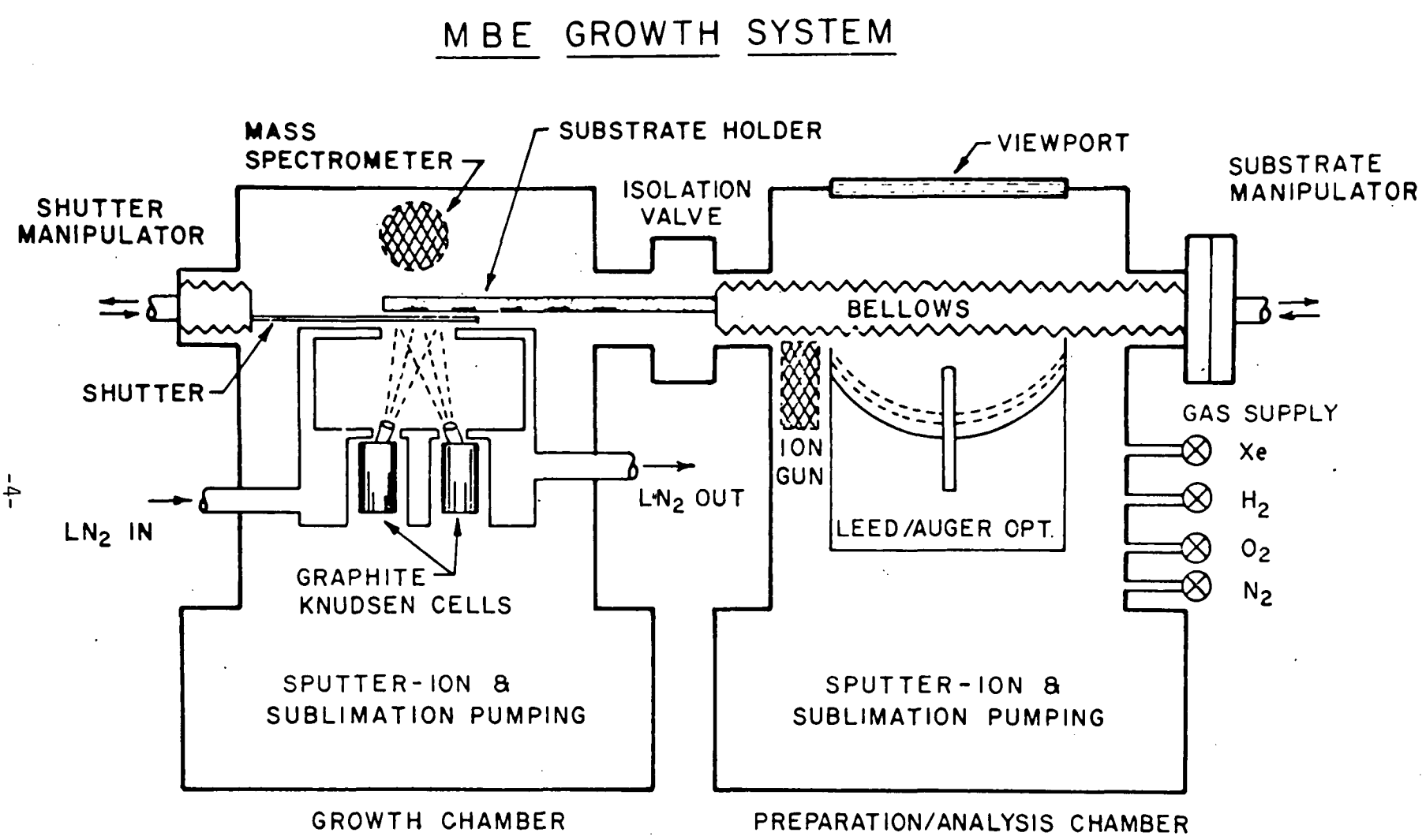

Figure 1. Schematic diagram of two chamber molecular beam epitaxial growth system

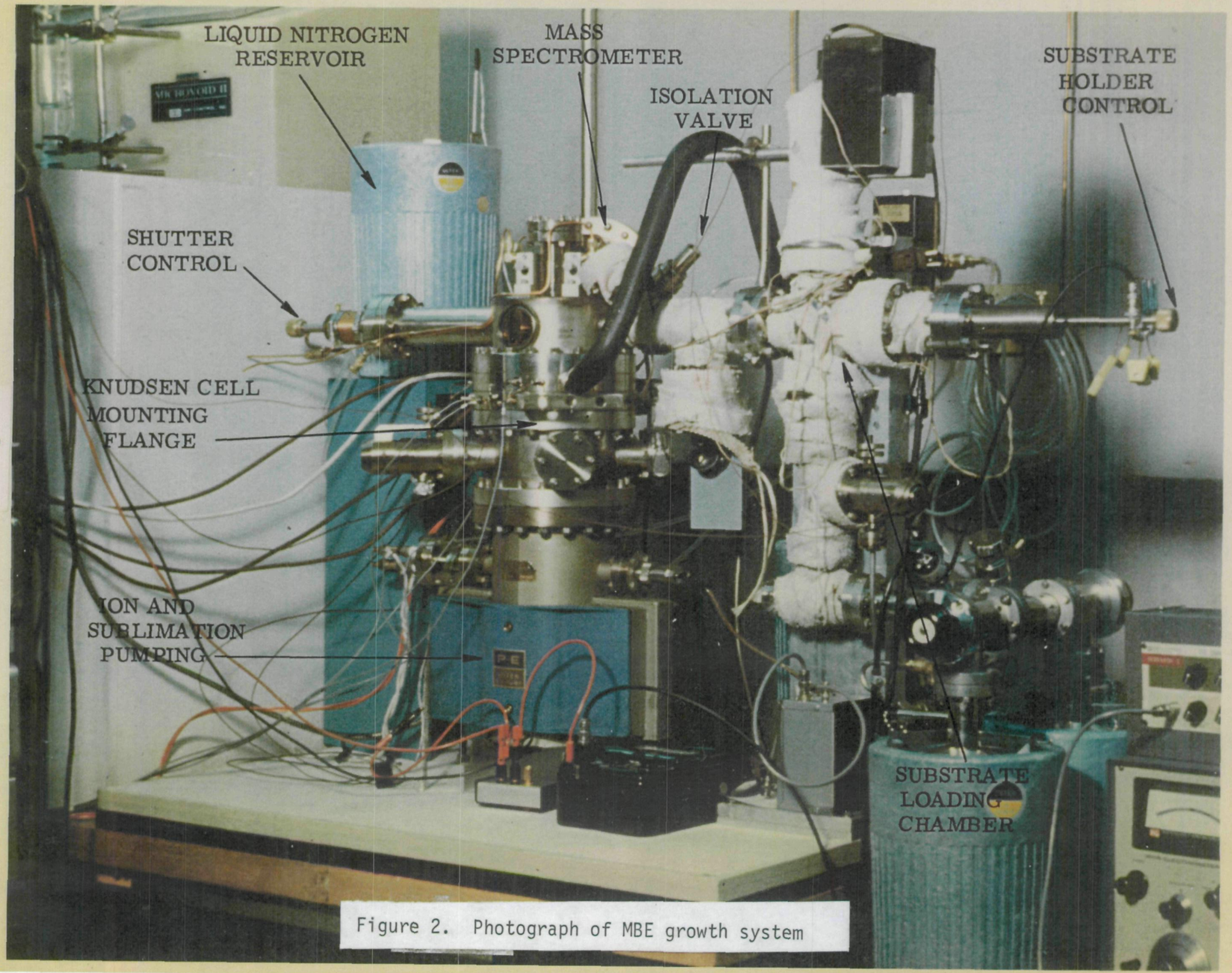

Figure 2. Photograph of MBE growth system

in the base. Figure 3 is a detailed drawing presenting the cell design. Figure 4 shows the entire source assembly, which has provision for as many as six sources, although we use only five for growth of (PhSn)Te.

Once a crystal growth procedure has been established in the research grower, device-oriented growth runs are carried out in a second "production" grower. The production system is identical to the research system except that it does not have the in-situ crystallographic measurements capabilities (LEED, Auger) and it does not have the quadrupole mass spectrometer. The sources, vacuum integrity, and temperature controllers are all identical. All the (PbSn)Te films which were actually fabricated into lasers were grown in the production system.

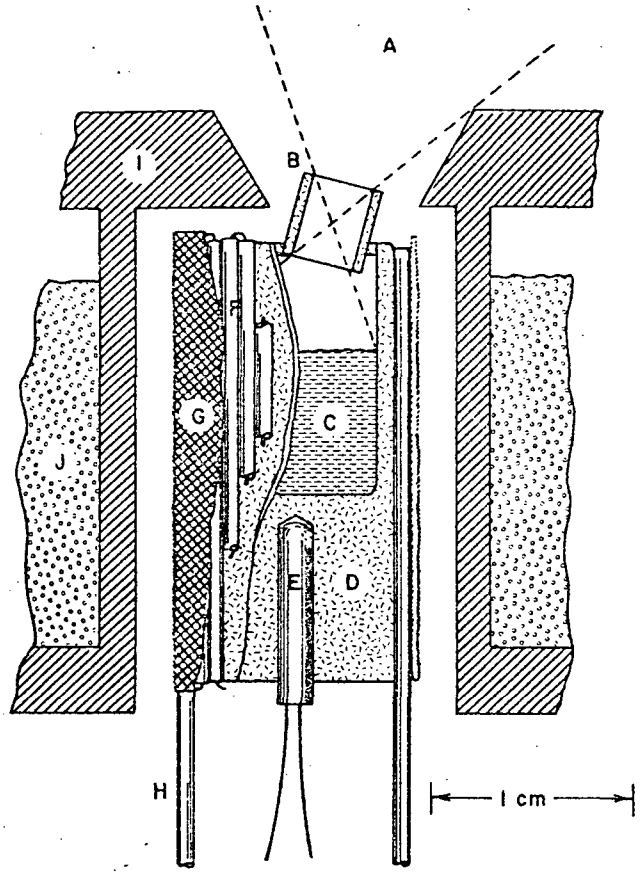

FIG. 3. Knudsen cell structure: A—molecular beam, B—collimating orifice, C—evaporant, D—graphite cell body, E—alumina thermocouple sheath, F—alumina-insulated tungsten heating wires, G—rippled Ta foil heat shield, H—alumina support rod, I—gold-plated copper shroud, J—liquid nitrogen.

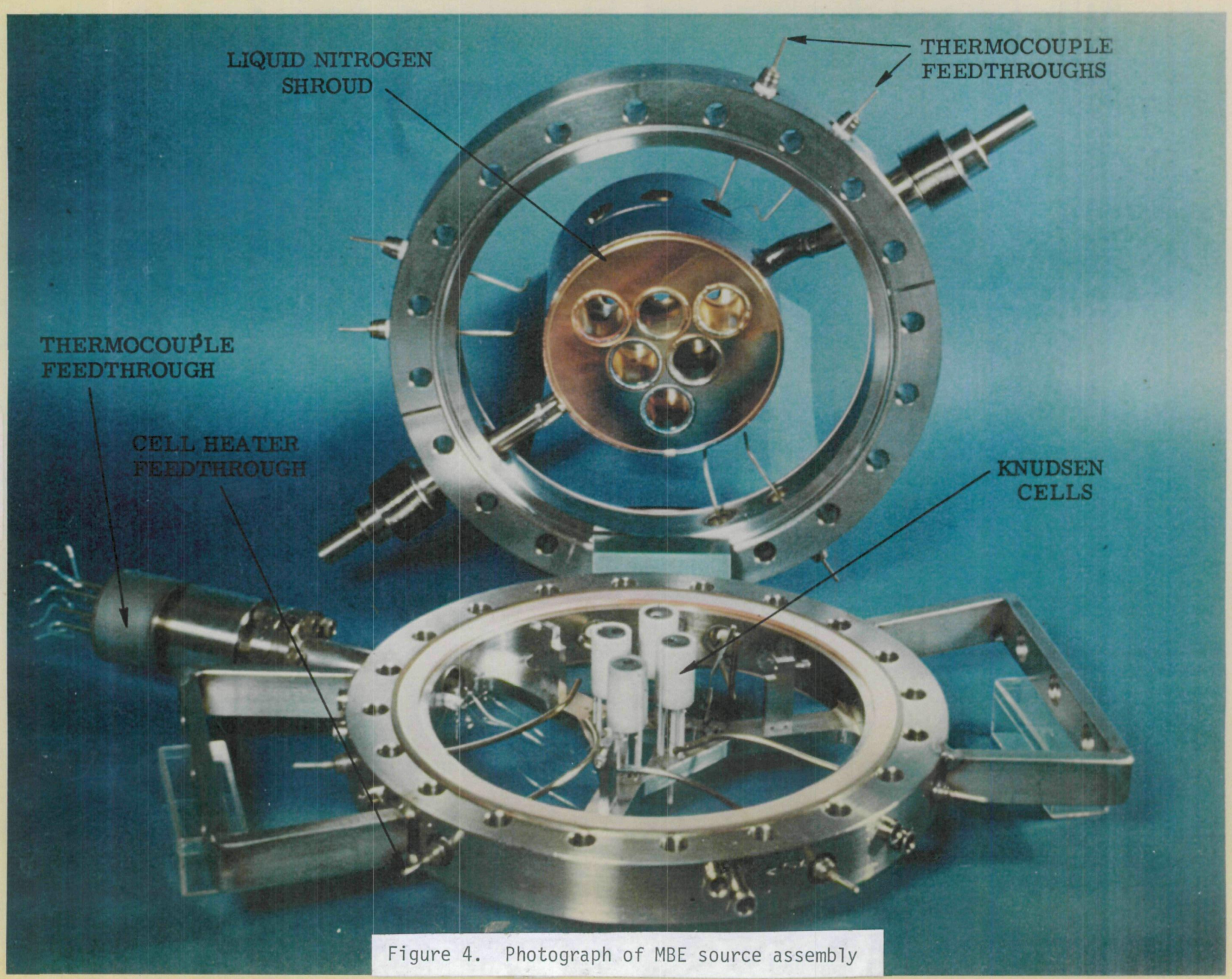

Figure 4. Photograph of MBE source assembly

2.3 Composition Control

Composition is a key issue for crystal growth, since the emission wavelength of a semiconductor laser is roughly determined by the band-gap, which in turn is determined by alloy composition and junction temperature. For $(Pb_{1-x}Sn_x)Te$ the dependence of Eg on temperature and composition is approximately the following:(1)

$$Eg \approx 0.19 - 0.543\ x + \frac{4.5 \times 10^{-4} T^2}{T + 50} \qquad (1)$$

where Eg is in electron volts, x is the mole fraction of SnTe, and T is the absolute temperature in ^{o}K.

In order to obtain reproducible and continuously variable composition, we grow $(Pb_{1-x}Sn_x)Te$ from independently controlled sources of PbTe and SnTe. Other approaches have utilized growth from the ternary alloy or growth from the individual elements. There are two problems with evaporation from a single ternary source. First, because the vapor pressure of SnTe is different from that of PbTe, the grown film has a composition which is different from the source, adversely affecting calibration. Second, as a source is consumed, its composition changes, adversely effecting reproducibility.

Growth from the elements Pb,Sn, and Te permits very precise control of the Pb/Sn ratio. A serious drawback to this technique is the requirement for maintenance of stoichiometry in the grown film. In the lead salts, like many compound semiconductors, stoichiometry variations affect electrical properties; indeed controlled stoichiometry variation is frequently used for junction formation. However, for growth via MBE, a difference of 10^{-4} between the incorporation rates of the metal and the non-metal can result in 10^{18} carriers per cubic centimeter. The approach at P-E has been to control composition by growing from independently controlled stoichiometric binary sources.

2.4 Carrier Concentration Control and Junction Formation

A common method for controlling carrier concentration and type (and hence, junction formation) is the variation of stoichiometry. In particular, metal vacancies (excess Te) make a grown film p-type, while excess metal makes it n-type. Extensive investigations at P-E have defined the limits of stoichiometric doping for MBE grown material, and it has not been possible to achieve adequate control of stoichiometry for laser fabrication by MBE growth. A particular problem is the achievement of heavily doped n-type material for ohmic contacts, as surface segregation of Pb droplets occurs before films can be made even 10^{18} n-type.[2]

Conversely, both Bi and Tl are incorporated as dopants to levels greater than 10^{19} cm^{-3}. Carrier concentration is determined by extrinsic doping, where Bi or Bi_2Te_3 is used for n-type doping and Tl is used for p-type doping.

The use of impurity doping therefore permits precise and independent control of both composition and carrier concentration. The $(Pb_{1-x}Sn_x)Te$ p-n junction structures are grown using four sources, principally:

1) stoichiometric, undoped PbTe
2) stoichiometric, undoped SnTe
3) Bi (or Bi_2Te_3) to provide n-type extrinsic doping
4) Tl to provide p-type extrinsic doping

In addition, there is a source of Te which is occasionally used for small stoichiometry adjustments.

2.5 Substrate Selection

(PbSn)Te lasers are traditionally grown on PbTe wafers cut from bulk-grown ingots. PbTe is difficult and expensive to prepare, and it is extremely difficult to handle. One of the unstated goals of this program was to improve device yield by utilizing a rugged and commercially available substrate for crystal growth.

BaF_2 has been used successfully by many researchers, including Perkin-Elmer, for the growth of high-quality Pb-salt infrared detectors[3]. It has also been used[4]

POTENTIAL SUBSTRATES FOR LEAD SALT CRYSTAL GROWTH

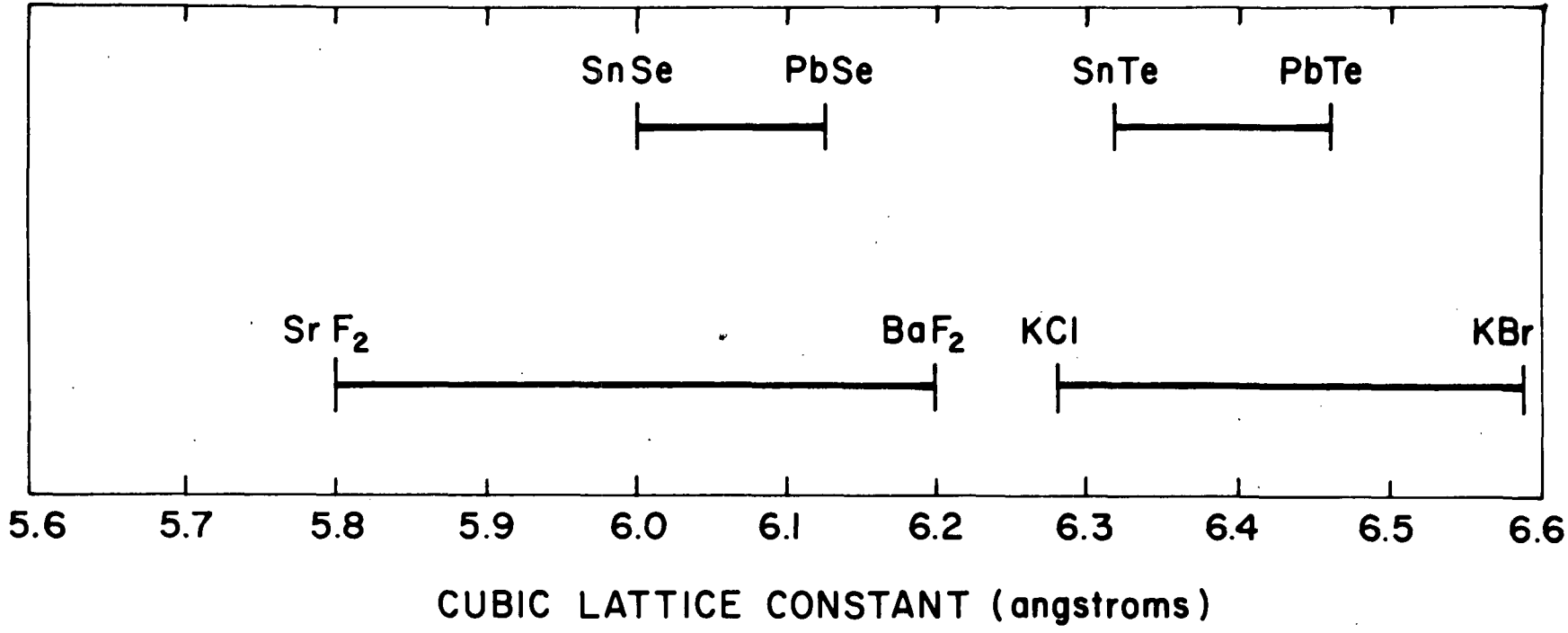

Figure 5. Lattice constants of potential substrates for lead salt crystal growth

to fabricate Pb/PbTe Schottky barrier lasers exhibiting low threshold current but restricted to operation at 12°K by thermal problems. These results were obtained despite the 3.7% lattice mismatch between PbTe and BaF_2. The mismatch between $(Pb_{.78}Sn_{.22})Te$ and PbTe is 0.51%.

Alkali halides have also been used as substrate for Pb-salt crystal growth. There have been no significance device results achieved on these substrates, however, primarily due to the large mismatch of their thermal expansion coefficients.

Figure 5 presents the range of cubic lattice constant as a function of composition for (PbSn)Te, $(BaSr)F_2$, K(ClBr) and (PbSr)Se. Lattice matching is possible either for (PbSn)Se grown on $(BaSr)F_2$ or for (PbSn)Te on K(ClBr). In light of the ready availability, excellent thermal properties, and history of good results, BaF_2 was selected as the substrate of choice for MBE growth of (PbSn)Te alloys.

3.0 Materials Preparation

3.1 Source Materials

Sources of PbTe and SnTe were synthesized[5] by vacuum melting stoichiometric ($\pm 10^{-4}$ atomic fraction) proportions of the high purity (grade 69) Pb,Sn, and Te, used as-received from Cominco-American. The sealed quartz ampules were heated to approximately 1200°C, rocked (to ensure mixing) and quenched in water to prevent segregation, which could occur during a slow cool down.

The polycrystalline ingot was then broken and ground, and the graphite Knudsen cells were filled with the resulting microstalline granules. After a cell was loaded, it was heated to a temperature 20°C above the temperature for crystal growth, for degassing purposes. Both the pressure in the growth chamber and the deposition rate on a quartz-crystal thickness gauge were monitored for the presence of outgassing impurities from the source. Typical chamber pressure during a growth run was less than 10^{-9} torr.

Before any doped junction films were grown, calibration films of uniform, undoped PbTe and (PbSn)Te were deposited on BaF_2 substrates. The carrier concentrations and mobilities measured on these undoped films are very sensitive indicators of electrically active impurities in the source material. If unacceptable results were obtained, the source was subjected to another degassing cycle. Typically, undoped films of (PbSn)Te are slightly p-type with 77°K mobilities in excess of 10^4. If two degassing cycles do not yield acceptable films, the source is emptied, baked, cleaned, and refilled.

The Knudsen cells for PbTe and SnTe were modified to reduce down time caused by refilling. The present cells are double the linear dimensions shown in figure 3, and contain enough material for approximately 40 film growths. Because the growth chamber is isolated from the loading chamber, the sources are kept at a background pressure of 10^{-10} torr between runs. Contamination of sources is not a problem for

a crystal grower which is kept moderately active, however, even at 10^{-10} torr, the source material becomes contaminated after several months of inactivity. The dopants were high purity Bi (or Bi_2 Te_3) and Tl, obtained from Cominco-American and loaded as-received into graphite Knudsen cells of the dimensions shown in figure 3. The dopants are typically 10^{-3} to 10^{-4} atomic fraction of the deposited film; thus dopant expenditure is no problem. However, the dopants are subject to contamination, particularly the metallic Tl, from exposure to air. Thus the dopant cells are thoroughly outgassed every time the growth chamber is exposed to air. The criteria for dopant cleanliness are threefold:

1) no time dependent increase in pressure should be seen when the source is turned on

2) deposition rate (measured) with quartz monitor)must be consistent with known vapor pressure as a function of source temperature

3) carrier concentrations and mobilities must be consistent with the body of dopant calibration data

3.2 Substrate Preparation

Monocrystalline BaF_2 of the highest available purity (optical grade) was obtained from both Harshaw and Optovac. The cleavage plane for BaF_2 is (111), and this plane has frequently been used for MBE growth, primarily because of the ease of substrate preparation. However, there are two serious drawbacks to the (111) orientation:

1) cleavage steps are almost unavoidable

2) the Pb salts prefer growth with the (100) habit

Perkin-Elmer has considerable experience growing on both (111) and (100), and the (100) orientation was selected for this program.

The as-received boules of (100) material were checked for proper orientation by Laue X-ray diffraction, sliced into 8mm x 10mm x 1mm wafers, and lapped to a rough finish on 3 micrometer SiC paper. Final surface finish was achieved by chemo-

mechanical polishing in an aqueous solution of ammonia and precipitated silica. The resulting surfaces were featureless under 1000x Nomanski microscope examination and gave LEED patterns immediately upon chamber evacuation. Brief heating to 450°C improved the contrast of LEED patterns, and this heat cleaning was always used before film growth.

A significant substrate selection problem arose during the course of this program. An important step in diode fabrication is wet-chemical etching of the (PbSn)Te with a solution of Br_2 in HBr. This process will be further described in the section 4.6.1 of device fabrication.

It was found that many films exhibited a high density of unetched bumps and lines as shown by figures 6 and 7. A dislocation etch (using the same etchant) was performed on the BaF_2 substrates, shown in figure 8. It was thus evident that an unetchable precipitate was forming along the defects present in the starting BaF_2 substrate material. Samples were sent to Skinner and Sherman (a consulting firm in Waltham, MA) who performed elemental analysis for Pb, Sn, and Te in a partially etched film. Their analysis showed (PbSn)Te in the smooth featureless regions, and only Te in the cosmetic defects. By analyzing the ridge illustrated in figures 9 and 10, they found the Te rich material extended into the unetched portion. Thus, one concludes that the Te precipitates during growth, since that region was not exposed to the chemical etchant.

From these experiments, we concluded that the microcrystalline structure (low angle grain boundaries and point defects) in the starting BaF_2 significantly affected device yield by inducing Te precipitation during film growth. Subsequently, substrates were selected by dislocation etching. It was found that Optovac material was of substantially poorer crystal quality than Harshaw, and all runs after March 1978 were carried out on Harshaw BaF_2.

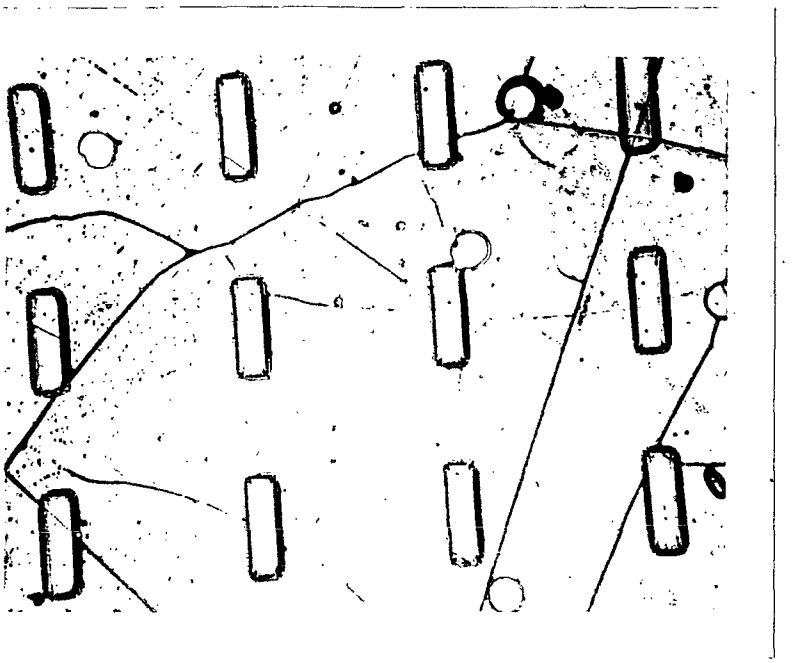

Figure 6. 50X photograph of etched (PbSn)Te film illustrating points and lines of unetched material interspersed between mesas protected by photoresist

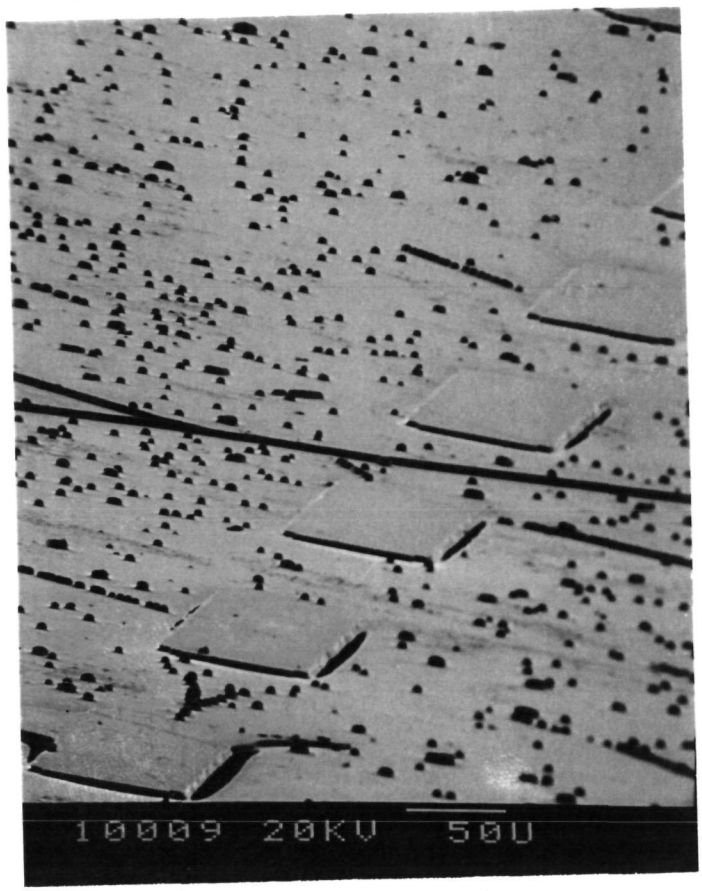

Figure 7 SEM photograph of the film from Figure 6 demonstrating the relief nature of the defects between the mesas

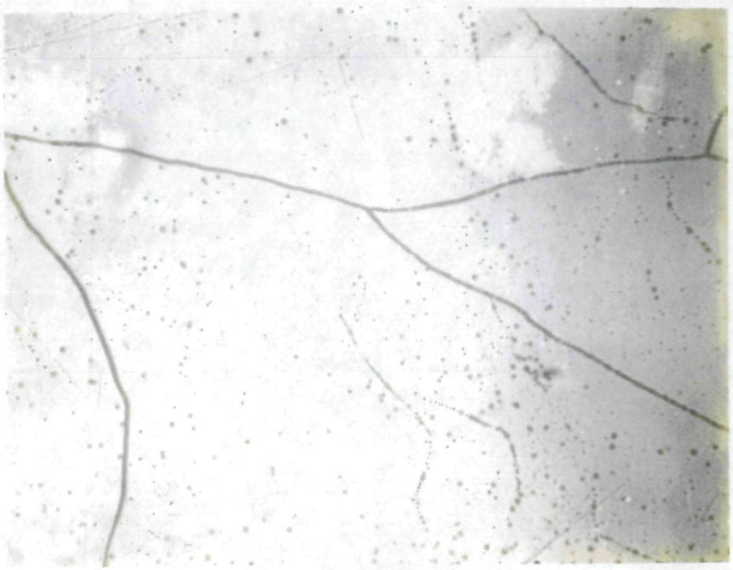

Figure 8 50X photograph of BaF_2 substrate after dislocation etch, revealing point and line defects in the substrate

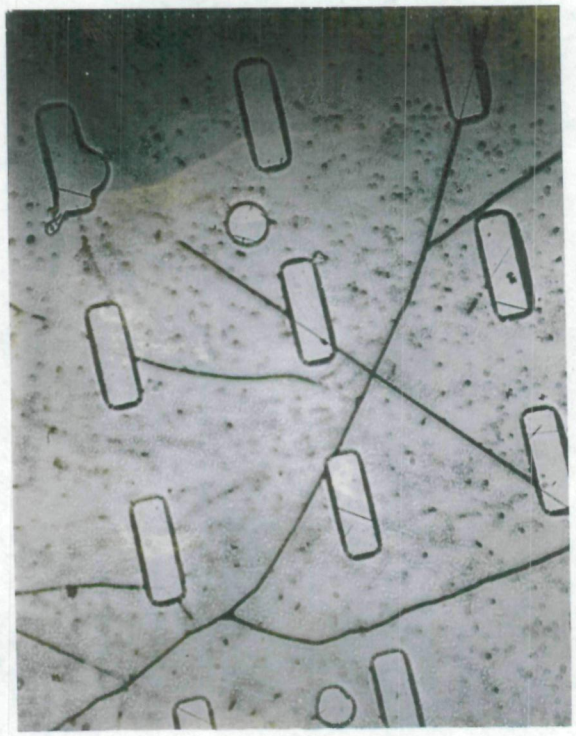

Figure 9. 50X photograph of (PbSn)Te film showing unetched ridges and bumps between .003"x .010" etched mesas.

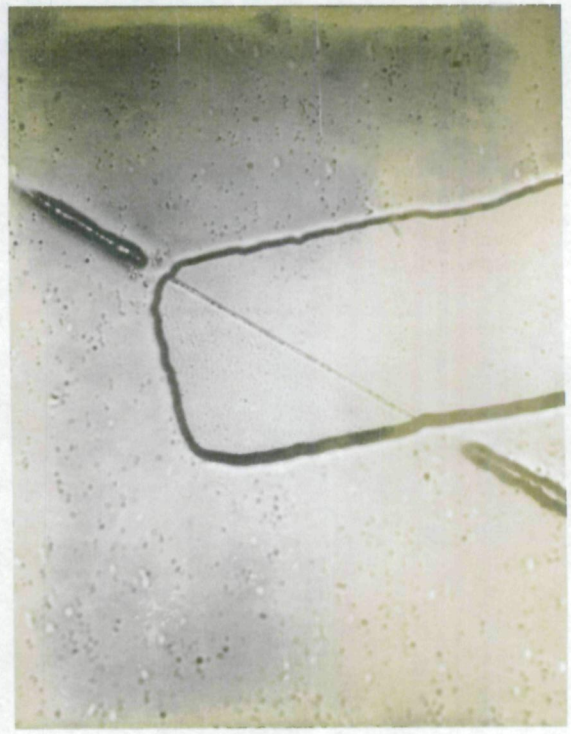

Figure 10. 500X photograph illustrating unetched ridge adjacent to mesa.

4.0 Device Fabrication

4.1 General Description

Figure 11 illustrates the significant operations in laser fabrication, starting with MBE film growth on a BaF_2 substrate and finishing with a bonded, electrically contacted laser. Although crystal growth is identified as only one of five milestone operations, the significance of crystal growth technology cannot be underestimated. Nor, on the other hand, can the importance of reliable and reproducible device processing be underestimated. In laser fabrication, there are very few quality control operations, other than visual inspection, which can be performed between crystal growth and final testing; and a device performs well only if every one of as many as sixty sequential operations is performed properly.

To a large extent, the flow of the device fabrication is dictated by the crystal growth process. For the purposes of this program, both the growth technique and the substrate were predetermined; and developing processing techniques for laser fabrication was a significant technical challenge, as there was an extremely limited world-wide experience base upon which to draw.

As depicted in figure 11, there are five milestone operations culminating in arrays of mesa diodes whose structure is illustrated in figure 12. First, of course, a multilayer vertical structure is grown by MBE on a BaF_2 substrate. The details of the vertical structure will be discussed in Sect.4.2 . At this point the wafer is an 8mm x 10mm x 1mm slab of BaF_2 completely covered by a single crystal of (PbSn)Te 8mm wide, 10mm long and 9um thick. In order to achieve adequate heat sinking to permit cw operation above $12^{o}K$, the film must be removed from the BaF_2 and bonded to an appropriate thermal expansion matched substrate.

This step was achieved by back surface metallization and a low temperature soldering operation to an OFHC copper block (see section4.4). The BaF_2 was then dissolved with a continuous directed stream of warm de-ionized water. Following

this operation, the wafer now consists of an 8mm x 10mm OFHC copper block, to which has been soldered the single crystal film grown in the first operation.

At this point individual Fabry-Perot cavities are formed photolithographically. The (PbSn)Te mesas are typically 75um wide, 250um long, and 9um high. They are isolated from each other electrically by a reverse-biased p-n junction, but they have a common electrical ground and heat sink. All that remains to form individual devices to contact the isolated top surface electrically. Because of the delicate nature of the (PbSn)Te crystal, direct contacting is extremely difficult; therefore a process was devised in which an insulating layer was deposited and contact windows opened. Metal was then deposited over the entire top surface and selectively removed from one face of the laser permitting the output radiation to escape. The structure is completed by fastening a contact wire to the top layer metallization beside the laser, thus avoiding the mechanical stress of a direct contact.

A very significant feature of this fabrication process is that it automatically affords mass production. A single film is 8mm x 10mm. The laser dimensions were the following:

Diode dimension	75um x 250um
Contact window	50um x 200um
Top metal contact pad	375um x 375um
Diode to Diode Separation	500um X and Y.

Thus hundreds of diodes can be fabricated simultaneously from a single growth run. Another feature of this fabrication technique is that it immediately lends itself to array fabrication.

PROCESSING STEPS IN LASER FABRICATION

1. FILM AS GROWN BY MULTIPLE SOURCE MBE ON BaF_2 SUBSTRATE
2. SOLDERED TO COPPER HEAT SINK
3. BaF_2 DISSOLVED WITH WARM WATER, FABRY-PEROT CAVITIES ETCHED
4. BaF_2 INSULATOR DEPOSITED, CONTACT WINDOWS OPENED
5. TOP METALIZATION DEPOSITED, REMOVED FROM EMITTING FACE, CONTACT WIRE BONDED AWAY FROM ACTIVE LAZER

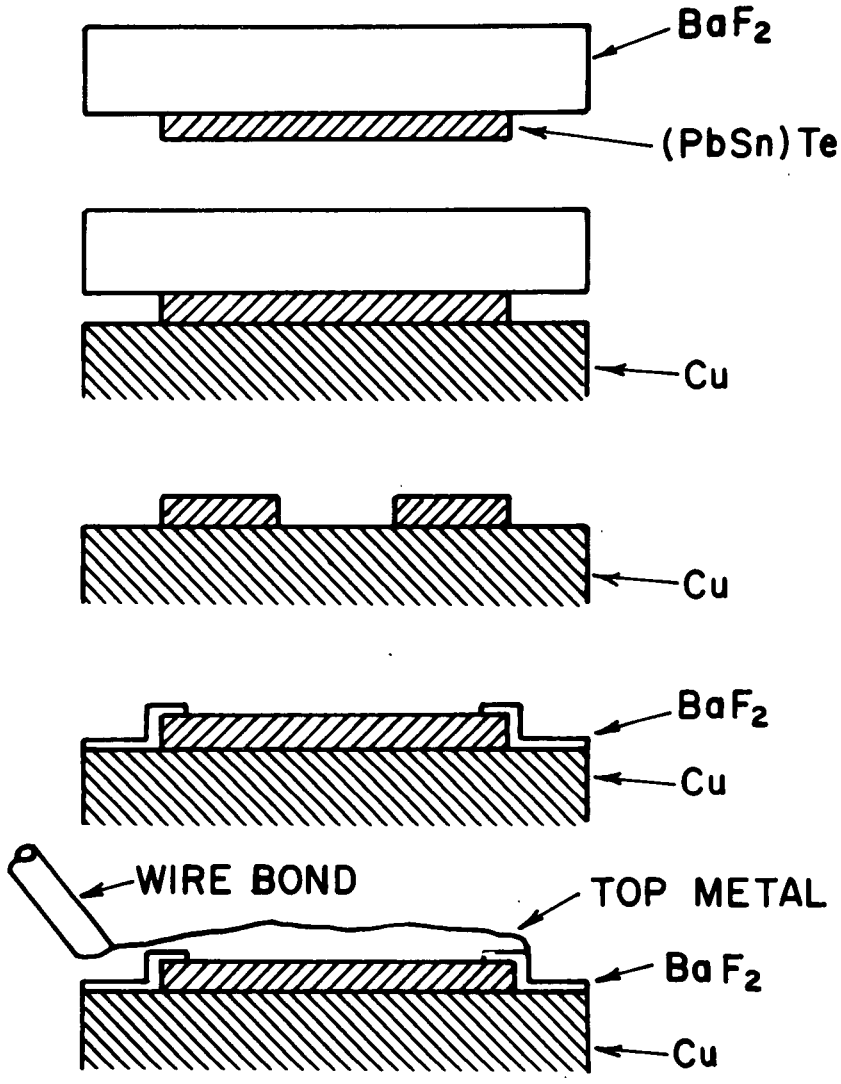

Figure 11. Processing steps in laser fabrication

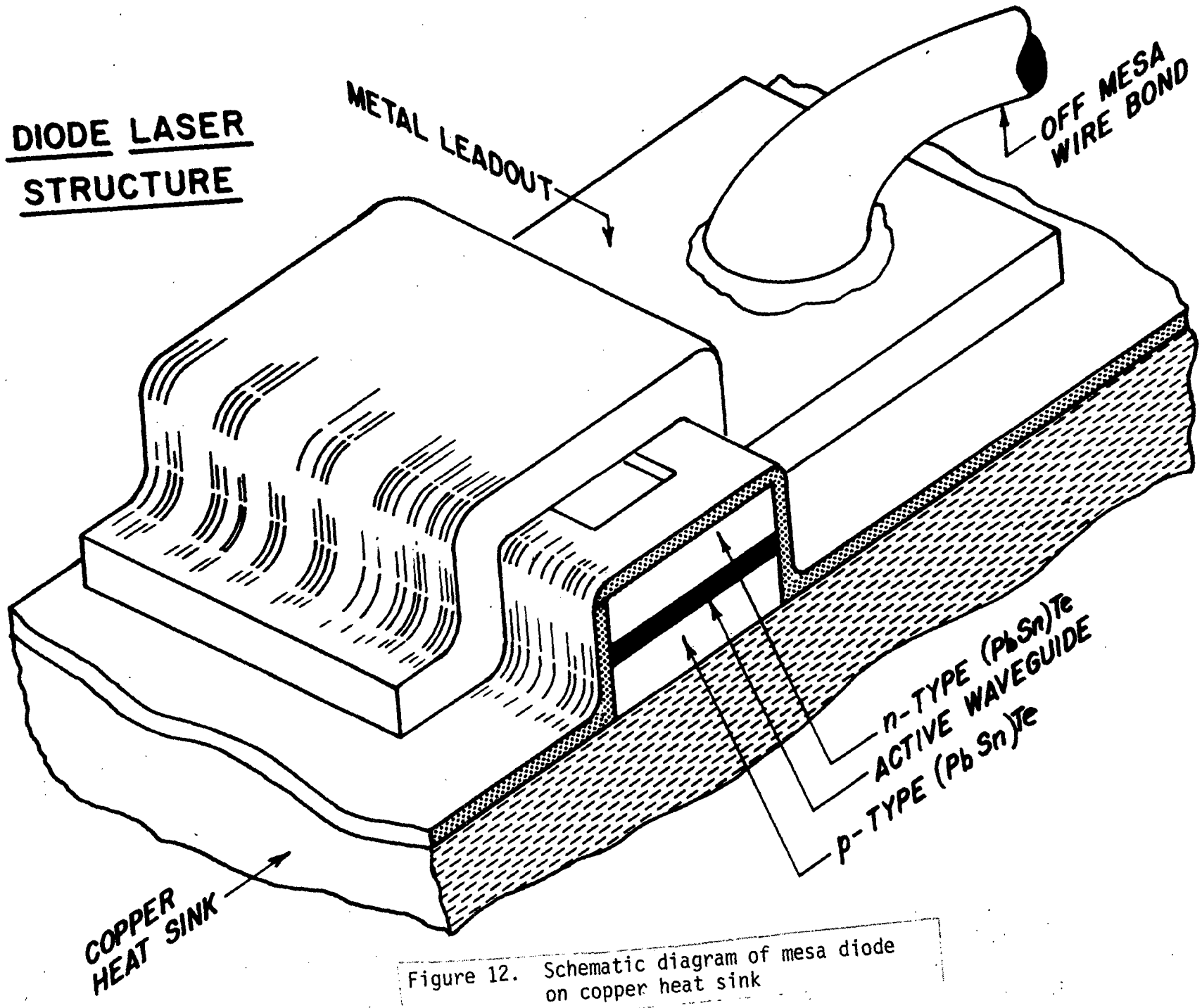

Figure 12. Schematic diagram of mesa diode on copper heat sink

4.2 Vertical Structure

Dependence of composition and carrier concentration on position along the growth direction defines the vertical structure of the film. These profiles, together with the crystallographic quality of the material, are the most important parameters for fundamental device performance. Device processing after crystal growth can certainly degrade performance; it is not difficult to make poor devices from good material. On the other hand, there is no process at all by which good devices can be made from poor material.

The vertical structure of the film must permit the achievement of four functions in the device:

1) it must be possible to form low resistance ohmic contacts to both sides of the p-n junction

2) it must be possible to conduct heat from the junction efficiently

3) injected carriers must be confined effectively within the active region of the device

4) radiation must be guided effectively along the active region.

Traditional bulk-diffused p-n junction lasers do not offer effective carrier confinement or waveguiding, although the material properties can be excellent. The devices typically afford excellent performance at low temperature, but have restricted tuning ranges due to rapid increase of threshold current with temperature. This problem is frequently compounded by ineffective heat sinking due to the unavoidable thickness of the bulk material and the very low thermal conductivity of the Pb-salts.

The most dramatic advances in the performance of III-V semiconductor lasers has been the introduction of lattice matched heterostructures affording controlled optical confinement and carrier confinement. There have also been good results with a variety of heterostructures in the IV-VI compounds; however, until recently, lattice matching was not possible, and crystallographic quality of the heterostructures is always questionable. Furthermore, it has been demonstrated both theoretically,[6]

and experimentally[7] that strong optical confinement and carrier confinement can be achieved with properly controlled carrier concentration profiles. Thus epitaxial homostructures can have the advantages of heterostructures, while eliminating the problems associated with a lattice mismatch at the edge of the active region of the laser. While carrier concentration profiles can be controlled in bulk-diffused devices[8], there are very substantial advantages for MBE growth of structures utilizing tailored carrier concentration profiles.

The laser structures grown for this program were all homostructures of $(Pb_{1-x}Sn_x)Te$, where the x value was selected according to the desired wavelengths. Three values of x were used in this program:

1) $x = 0.22$ — this composition is appropriate for 14um detectors operating at 77°K. Films were grown with x = 0.22 as calibration checks on the growth system, since this is a composition for which there is considerable experience

2) $x = 0.19$ — this composition provides 14um emission at 12°K. As originally structured, the goal of this program was widely tunable diode lasers in the 8-14 um range

3) $x = 0.15$ — this composition was selected to obtain the specific target wavelengths of 894 and 1015cm^{-1} at a heat sink temperature of 20°K.

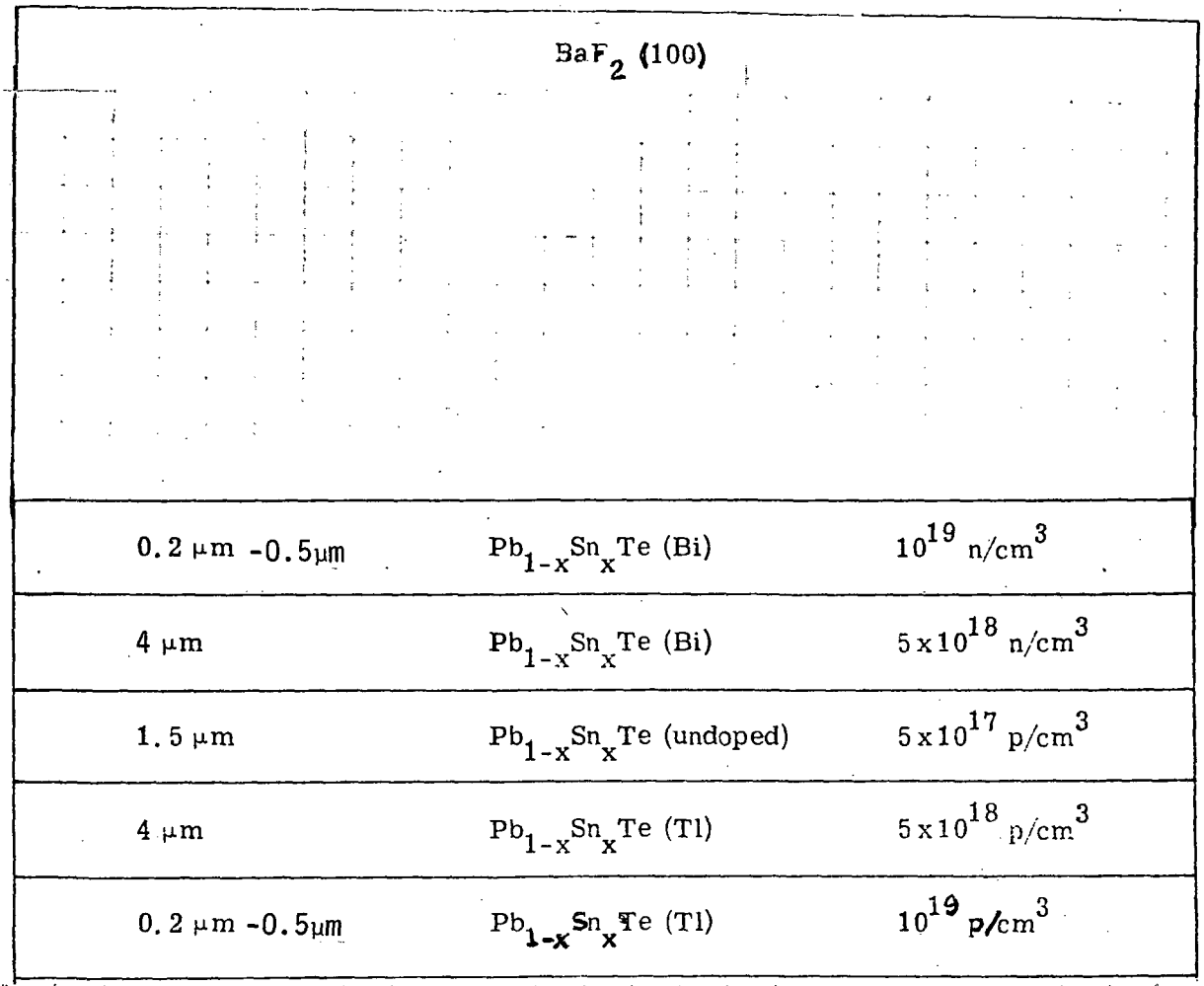

Figure 13. Cross-section of $Pb_{1-x}Sn_xTe$ homostructure utilizing carrier concentration gradients for optical confinement and carrier confinement

The carrier concentration profiles varied slightly from growth to growth. A typical target profile is illustrated in figure 13. These structures are symmetric, and each of the five layers address a specific device requirement. The heavily doped cap layers, top and bottom, are intended to facilitate ohmic contacting. The carrier concentration in these layers should be as high as possible. The value of 10^{19} cm^{-3} is roughly half the maximum value which we can achieve without a reduction in the incorporation rate of the extrinsic dopants, and is therefore a dopant level for which crystal quality is still reasonably good. It is critical, particularly for the first layer grown, to achieve high quality growth, since the remaining structure is deposited upon that initial layer.

Because the device structure (figure 12) provides heat sinking primarily through the soldered surface, it was decided to place the higher resistance contact on that surface. For the Pb-salts, it is generally the case that the p-layer contact is more difficult to form. For this reason, the Bi doped (n-type) layers were used to initiate growth. The first 4μm thick cladding layer acts as a crystallographic buffer region between the initial heavily doped n-layer cap and the lightly doped active region. The thickness of this layer is selected to assure high quality crystal in the active region without building up excessive thermal resistance. The carrier concentration is not critical; it must be substantially higher than that of the active region, but it should not be so high as to introduce excessive free-carrier absorbtion. Typical values were 3×10^{18} - 5×10^{18}.

The active region is not extrinsically doped, since the as-grown undoped material is typically 3-8 x 10^{17} p-type (depending upon growth parameters and alloy composition). The greater the SnTe content, the greater the p-type conductivity of the undoped layer. The transition from the cladding layer to the active layer affords both optical confinement and carrier confinement; the carrier confinement arises from the potential difference caused by the concentration gradient while the

optical confinement arises from free-carrier contribution to the index of refraction[1,6,7]. The Tl doped cladding layer is roughly symmetric to the Bi doped layer in order to provide a symmetric waveguide with fairly simple mode properties. Finally, a heavily doped p-type cap is deposited to provide ohmic contact.

Growth rates were typically 4um/hr at a substrate temperature of about 420°C. Temperature control of insulating substrates under vacuum is a difficult problem. The substrates were heated by an iron block contacted to the back of the substrate with liquid tin. The block temperature is read to ±0.5°C by a chromel/alumel thermocouple spot-welded to the back of the block, and this signal is coupled through a proportional controller to a quartz/halogen lamp heater external to the chamber. The temperature at the growth surface has been computed to differ from the thermocouple temperature by at most 2°C.

The growth rate and substrate temperature are not critical. The upper limit to the substrate temperature is determined by the re-evaporation rate of the growing film. Growth at rates as low as 1um/hr may be carried out up to 420°C before re-evaporation becomes as high as 10% of the growth rate. Higher temperature also causes square thermal etch pits . At a rate of 4um/hr and 420°C, these effects are insignificant. It has also been observed that it is preferable to initiate growth at a slightly lower temperature. Typically, a run will be initiated by 0.1um grown at 1um/hr and a substrate temperature of 350°C. Subsequently, the rate is increased to 4um/hr and the substrate temperature raised to 420°C. Upon completion of growth, the heating block is raised from the BaF_2 to avoid cracking. A typical cool down rate is 15°C/min.

4.3 Back Surface Metallization

The back surface metallization is applied to the heavily doped p-type (PbSn)Te. For most of the work encompassed by this program, the metal was vacuum deposited in a chamber different from the growth chamber, and therefore required exposure of the grown (PbSn)Te to ambient air. Electron beam evaporated films, particularly of the refractory metals, were of much better quality than thermally evaporated ones. There are many constraints imposed upon this deposited metal. First and foremost, it must provide an extremely low resistance ohmic contact to the p-type (PbSn)Te. Series resistance in the contacts has been one of the dominant failure mechanisms in these devices. Because the lasers are typically operated at 0.5-2A, I^2R heating in the contacts can lead to substantial heat input to the diode, and this heat quenches the lasing through the strong temperature dependence of the threshold current. According to the classical theory of contact formation, metals with high work functions are used to contact p-type semiconductors, and metals with low work functions are used on n-type material.

From a device fabrication standpoint, the metal must achieve much more than this. It must possess the following properties:

1) form stable low resistance ohmic contact to p-type PbSnTe
2) adhere reliably
3) permit reliable mechanical, electrical, and thermal contact to Cu heat sink
4) resist chemical attack by etchants used to define mesas in PbSnTe
5) resist diffusion of indium

The high work function metals most commonly used are Pt and Au. Unfortunately, neither of these materials is particularly adherent when vacuum deposited on semiconductor surfaces. A further problem is encountered when Au is used in conjunction with indium. Indium has been known for a long time to diffuse rapidly through gold at room temperature. It was thus suspected that a possible cause of the well publicized room-temperature shelf-life problem was indium diffusion. Since In

is an n-dopant in the lead salts, it would tend to counterdope the p-type semiconductor surface and raise the contact resistance.

A great deal of process development time, documented in the monthly reports, was expended developing an acceptable p-layer contact material. Table I summarizes the properties of metals tried as ohmic contacts. The best results were achieved with nickel or platinum as the p-layer contact. The metallization for the cw lasers delivered consisted of a 1000Å film of Pt followed by 3000Å of Cu, to render the film solderable. These devices were defined by wet chemical etching, and the Pt metallization was required for its chemical resistance. The Pt/Cu/Solder metallization scheme was not reproducible in terms of its mechanical properties, however.

A far preferable process for mechanical adhesion utilized a 600V, 30sec ion-milling clean up operation on the p-layer, followed immediately by evaporation of 750Å of Ni. This Ni layer was adherent and reliably solderable. Ni was not sufficiently resistant chemically, however, and was used only on devices which were defined by ion-milling.

A third process which was employed during the last three months of the program consisted of an in-situ deposition of approximately 100Å of platinum on the as-grown p-type material. This platinum deposition was accomplished by flash evaporation from a filament in the growth chamber, and the purity of the deposited material was not verified. The in-situ platinum deposition was attempted in order to utilize the metal with the highest possible work function on the cleanest possible (PbSn)Te surface. After Pt deposition, the films were removed from the growth chamber and an additional 750Å of Ni and 1.5um of gold were deposited. These films were reproducibly solderable and were excellent mechanically; there was some question about the quality of the electrical contacts, which may have been due to impurities in the flash evaporated platinum.

TABLE I Properties of Vacuum Evaporated Contact Metals for (PbSn)Te

Metal	Work function (eV)	Adhesion	Solderability	Chem. Resist.	Mech. Stress
Gold	5.1	poor	good (but tricky)	fair	good
Platinum	5.65	poor	poor	good	poor
Palladium	4.85	poor	poor	fair	poor
Nickel	5.15	fair	good (but tricky)	fair	fair

4.4 Back Surface Soldering

The requirement of substrate removal places serious constraints on the bonding of the film to the heat sink. A strain-free mechanical, thermal, and electrical bond must be established between the metallized (PbSn)Te and the copper block. Bonding agents used included indium, cold weld, silver filled epoxy, and numerous Pb-Sn-In alloy solders. The cold weld experiments failed to achieve reliable bonds over a sufficient area. The epoxy successfully bonded the film, but the (PbSn)Te surface was seriously cracked and strained after substrate removed, probably due to an uncontrollable volume change in the epoxy.

There are numerous candidate solders which could be suitable for (PbSn)Te. The solder should melt at a low temperature, in order to avoid thermal stress during cool down. On the other hand, the melting temperature should be above 100°C since the BaF_2 is removed in heated, flowing de-ionized water. The solder should have reasonable low temperature thermal conductivity, should be malleable, and it should be adherent. Finally, if the solder contains In, it can be used only with a barrier metal to prevent In from reaching the p-type (PbSn)Te.

The solder which gave the best results, consistent with all these constraints, was a 50/50 In/Sn alloy obtained from Indalloy. The copper blocks were plated with nickel to prevent corrosion, and the solder was premelted on the copper block, using the flux recommended by Indalloy.

The soldering was carried out on a temperature controlled hot plate, in air, at 125°C. A special aluminum fixture was designed to hold both the BaF_2 and the Cu block next to each other and tilted 45° to the plane of the hot plate. When the solder melted and began to flow, the BaF_2 was lifted with tweezers and pressed against the molten solder, starting at the bottom and squeezing the excess solder and flux out the top. The tilted fixture and squeezing operation are essential to achieve void free bonds over the full 8mm x 10mm surface. Any horizontal technique invariably leaves pockets of air and flux on the molten solder. Once the

BaF_2 was soldered to the copper, the Al fixture holding them was removed from the hot plate and allowed to air-cool. A better process would invoke a controlled and optimized cool-down. If the film is cooled too rapidly, thermal stress results. If the film is cooled too slowly, the solder eventually dissolves off all of the metallization on the PbSnTe, and instantly loses all adhesion.

4.5 Substrate Removal

BaF_2 is very slightly soluble in water. The limiting process for the removal of the BaF_2, however, is not the solubility limit, but the rate of dissolution. Thus, while the saturated solubility decreases with increasing temperature, the rate of removal increases.

The substrates were removed by holding them under a stream of heated (about 60°C) deionized water. Even after carefully wire sawing the residual BaF_2 to a thickness of about .005", this process took two days. This became a very reliable process, and films were consistently and reproducibly soldered to copper heat sinks and separated from the BaF_2 growth substrate. Dislocation etching, microscopic analysis, and x-ray diffraction confirmed the crystallinity of these transferred films. Figure 14 illustrates the excellent cosmetics of the transferred films after substrate removal.

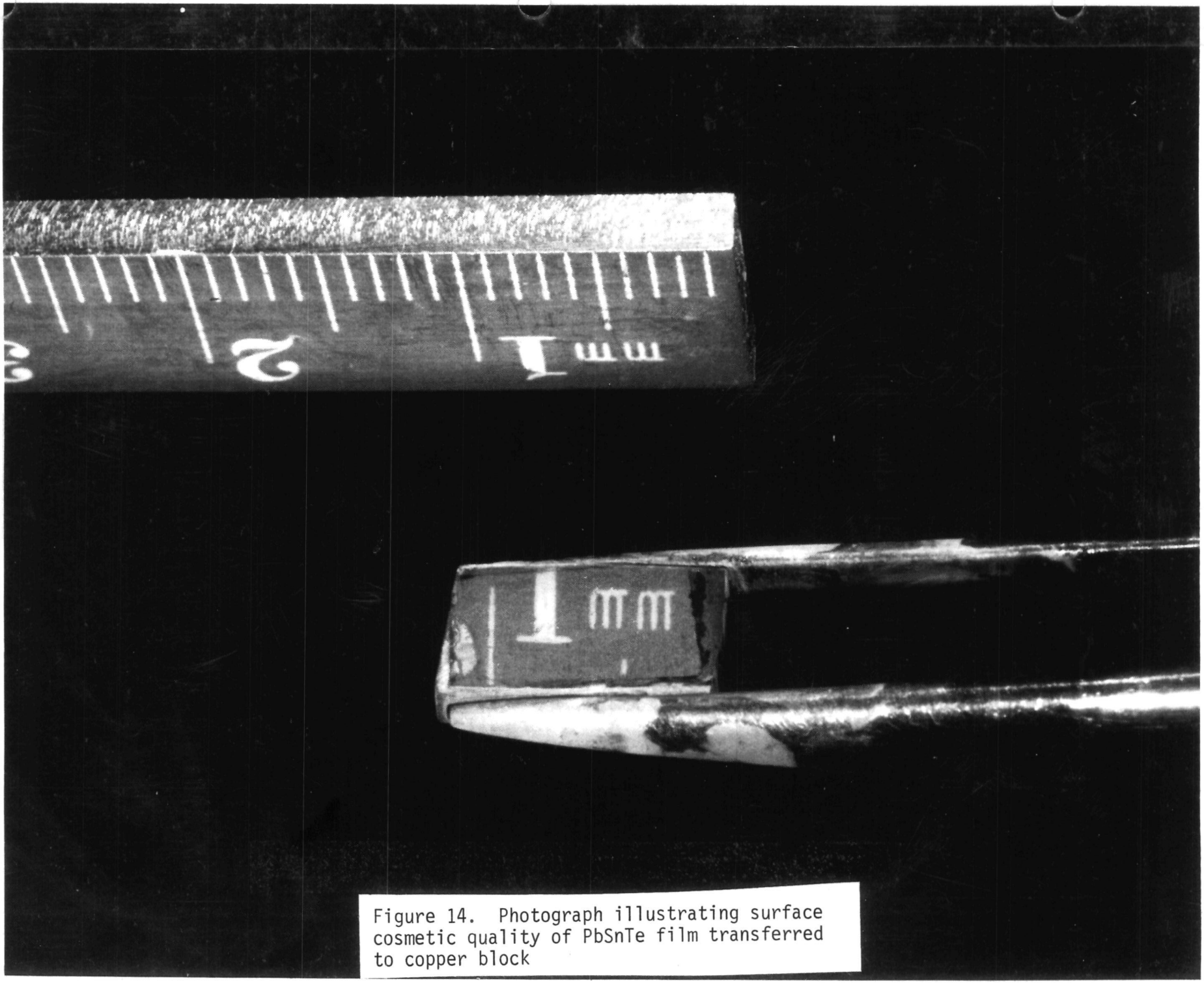

Figure 14. Photograph illustrating surface cosmetic quality of PbSnTe film transferred to copper block

4.6 Fabry-Perot Cavity definition - Mesa etch

4.6.1 Wet Chemical Processing

In the initial phase of this program, selective wet chemical etching was used for all photolithographic pattern definition. Two different chemical etchants were used:

1) "Fast etch" consisted of 2%Br_2/HBr
   Etch rate about 10μm/min, frequently leaves unremovable surface stain. Will not leave unetched ridges

2) "Slow etch" consisted of 1%Br_2/HBr
   dissolved 1/3 in de-ionized H_2O
   Etch rate about 1um/min. Will not leave surface stain if constantly stirred. Will leave unetched ridges in films deposited on $BaF_2$of poor crystal quality. Used as dislocation etch for (100)BaF_2.

All photolithography was done with Shiply 1350J, a positive photoresist. Exposures were performed in a modified Kulicke and Soffa model 686B precision mask aligner, for which special fixturing was designed to prevent direct contact of the photomask and the (PbSn)Te films. This fixturing was essential, due to the very fragile nature of the films.

Initial experiments demonstrated high quality mesa definition using the slow etch on (PbSn)Te films as-grown (still on the BaF_2 substrate). Contamination-free vertical walls were readily obtained, as illustrated by the scanning electron micrograph in figure 15. These results confirmed the results obtained by Weber and Yeung[4] who first reported etched cavities of PbTe on BaF_2. The excellent vertical profile arises from the undercutting of the Pb-salt film as it is held between etch-resistant photoresist and BaF_2.

Reproducing these excellent etching properties on (PbSn)Te which had been transferred to metallized copper heat sinks proved to be an extremely difficult task. The most significant problems were related to adhesion and chemical resistance of the p-layer contact metallization. It was found that both the OFHC copper and the In/Sn solder were very rapidly attacked by the etchants employed for patterning the (PbSn)Te. Furthermore, the exposure of the etchant to any etched metal resulted in redeposition

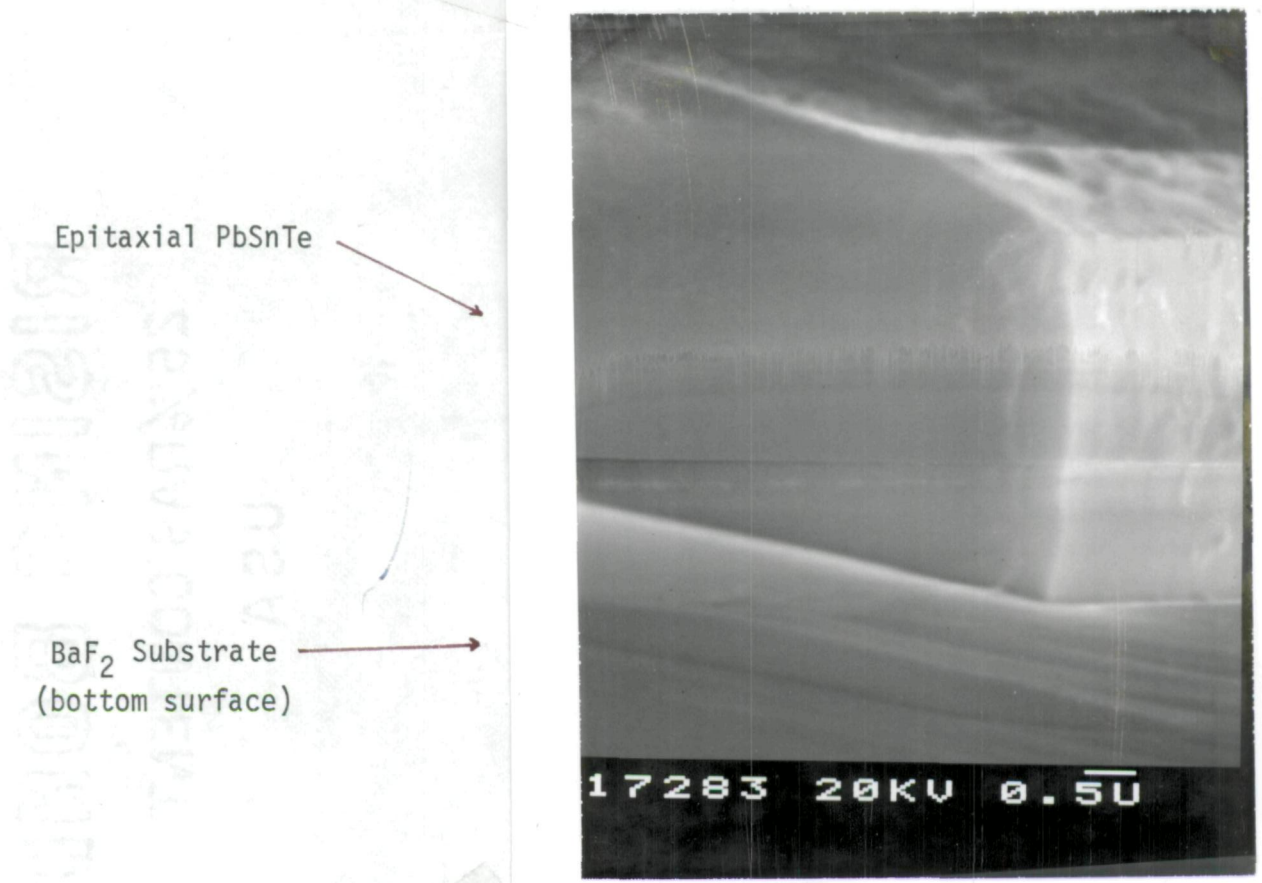

Figure 15. Corner of rectangular mesa etched in epitaxial PbSnTe film. Etch has undercut both the defining photoresist film at the top surface (not shown) and the BaF_2 substrate at the bottom surface, resulting in a flat perpendicular face.

of material on the laser faces. Particularly serious contamination occurred with copper or indium.

The requirement for undercutting to define vertical walls forced the p-layer contact metal to be in prolonged contact with the $Br_2/HBr/H_2O$ chemical etchant. Any delamination of this thin metal layer, caused either by mechanical strain or imperfect solder adhesion, exposed portions of the In/Sn solder to the etchant. The solder was very rapidly attached, ruining the mechanical integrity of the film and frequently depositing contamination on the exposed (PbSn)Te. Of the contact metals enumerated in Table I, only Pt proved an acceptable chemical barrier. Even with Pt as the p-layer contact, it was not possible to obtain truly vertical sidewalls on the Fabry-Perot cavity. The sloping sidewalls result in a misaligned cavity and probably degrade device performance. Figure 16 is a scanning electron micrograph showing a side view of a laser die. The chemical etch was halted when the operator began to observe evidence of solder erosion in one portion of the film. Figure 17, a more greatly magnified view of the same scene, illustrates both the sloped sidewall (caused by incomplete etching) and the cracked metallization which forced termination of the etch.

Despite the difficulties associated with wet-chemical etching, lasers defined wet-chemically operated cw (with admittedly low out put power of 10-20uw) and were delivered.

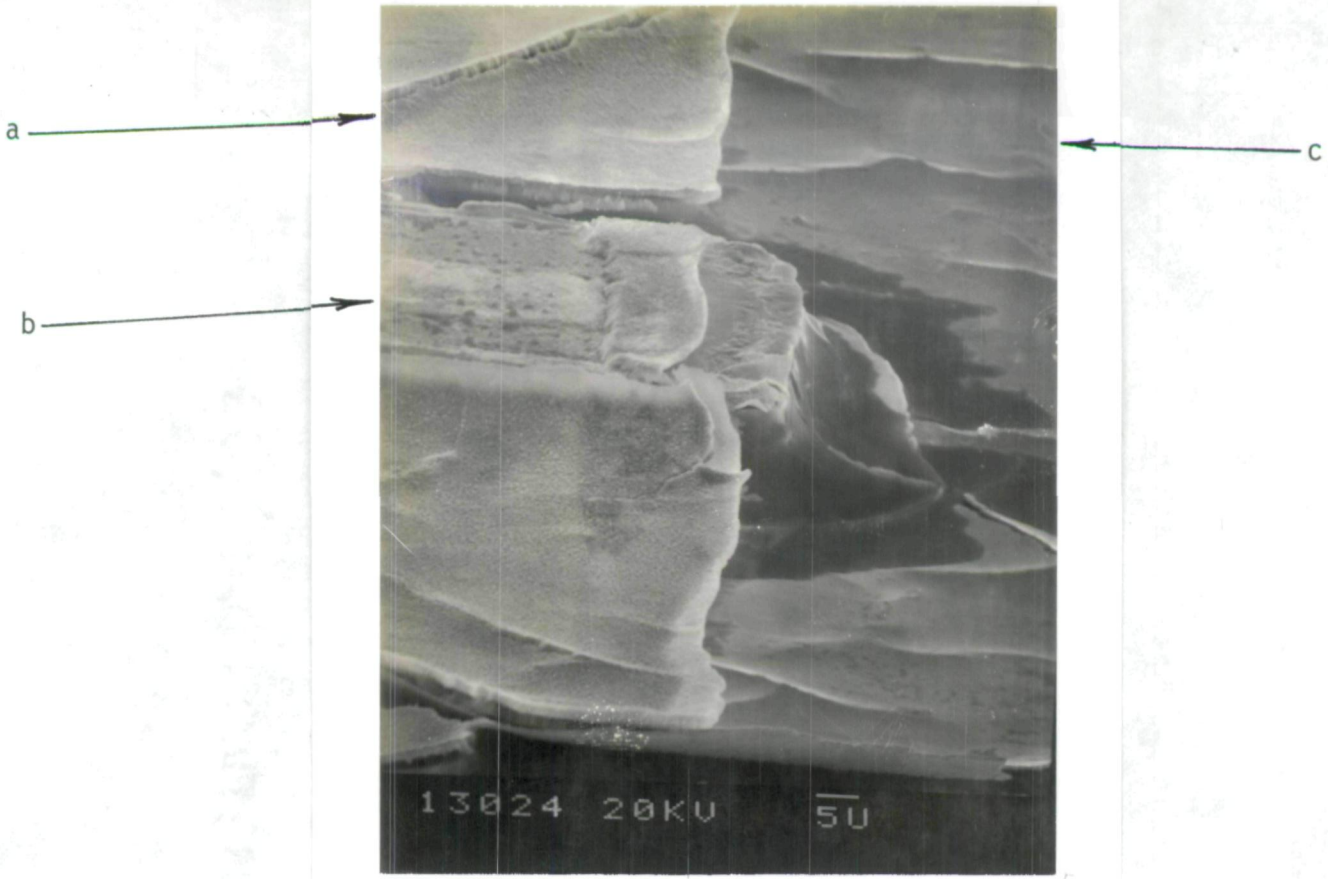

Figure 16. Side view of laser die. Significant features are
a. Metal bonding pad for top contact
b. Contact window opened in deposited BaF_2 insulator
c. Platinum metallization

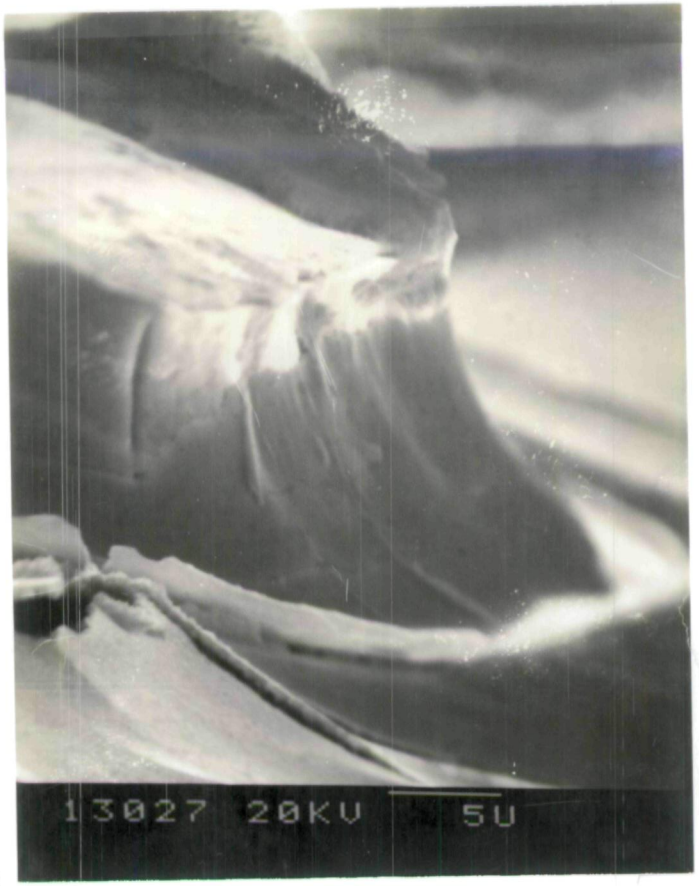

Figure 17. Magnified view of emitting face of laser. Dark portion is deposited BaF_2. Special attention is called to the cracked metallization evident in the foreground.

4.6.2. Ion Milling

An alternative approach to wet chemical processing employed a Veeco Argon Ion milling apparatus for mesa definition. This equipment was available only for the last four months of the program, and it yielded extremely promising results. A typical ion-milling operation was carried out with the argon ion beam of 1mA/cm^2 accelerated with a 600V potential and incident at 30^o to the substrate normal. The etch rate for (PbSn)Te was about 0.2um/minute under these conditions. This is a very high rate for ion-milling, and permitted the formation of excellent etch profiles without excessive erosion of the photoresist. Figures 18-20 are scanning electron micrographs demonstrating both the outstanding edge definition and the excellent yield obtained by ion-milling.

The only drawback to the ion-milling procedure is the difficulty of photoresist removal after prolonged exposure to the ion beam. This is a particularly severe problem if the resist is too thin. Before exposure to ion-milling, the resist must be examined, with particular attention paid to thinning at the edge of a line. If resist thickness is maintained all the way to the edge, the sample can be ion milled. Heat sinking during this operation is critical. The substrate is held to a water-cooled copper block by means of Apiezon vacuum grease. Care must be taken to make thermal contact across the entire surface of the sample, carefully squeezing the grease with a technique similar to that used for the soldering operation. If these precautions are taken, the photoresist can be removed with warm acetone after exposure to as much as 45 minutes of ion-milling.

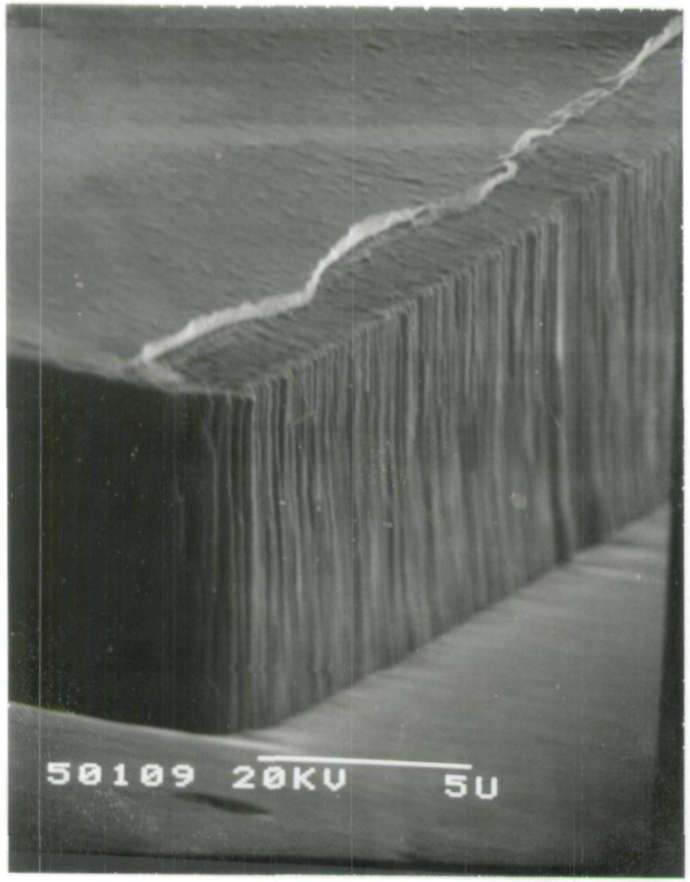

Figure 18. Magnified view of ion milled end face after photoresist removal.

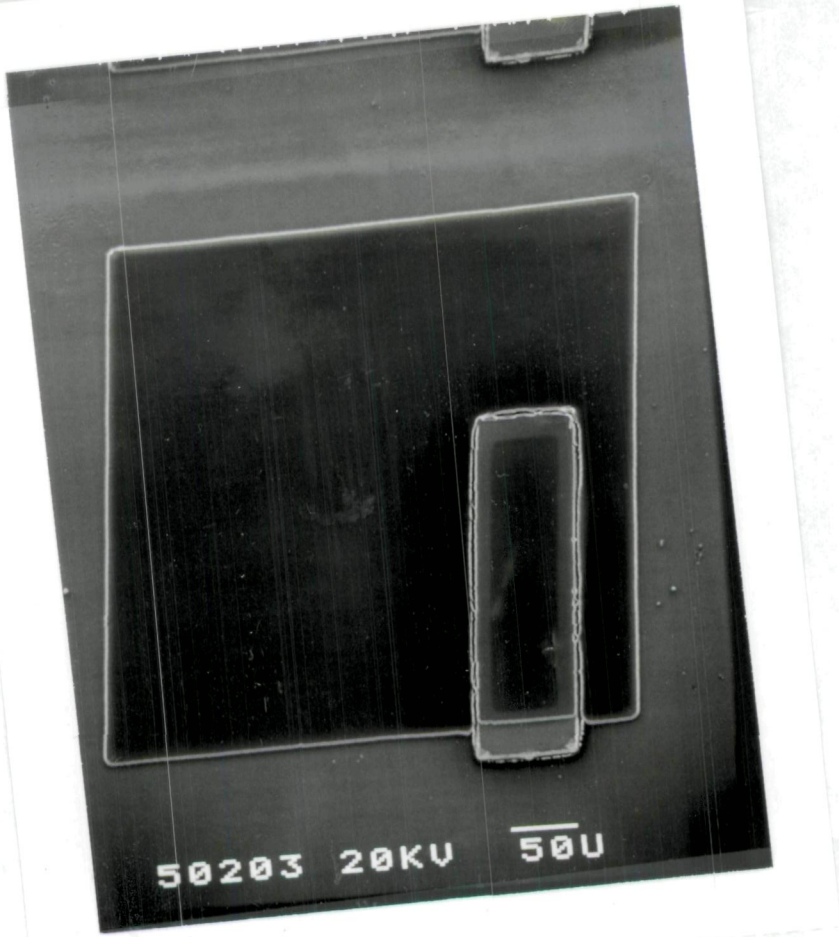

Figure 19. Scanning electron micrograph of all ion-milled structure.

Figure 20. Scanning electron micrograph illustrating high visual yield of ion-milling process.

4.7 Top Metallization

4.7.1 Contact Windows

In order to achieve off-mesa wire bonding, it was necessary to isolate the top metallization from the back surface metal which was exposed by the mesa etching process. The insulator must be adherent and must not be subject to thermal fatigue with cycling to cryogenic temperatures. Because of its excellent thermal expansion match both to (PbSn)Te and to copper, BaF_2 was used for this insulating layer.

The BaF_2 was vacuum deposited from a thermal source. In order to assure complete coverage, the substrate was tilted and rotated during deposition. Typical film thickness was 0.2um-0.5um. If the films were too thin, they did not provide complete coverage; excessive thickness led to cracking.

After deposition, windows were opened in the BaF_2 to permit electrical contacting to the mesa. These windows were 50um x 200um, and were defined either by etching (using water as the etchant) or by lift-off. The lift-off procedure was far superior. In this process a photoresist plug was defined on the mesa top prior to the BaF_2 deposition. If the resist had sharp edges and was significantly thicker than the deposited BaF_2 (typical resist thickness was 2um) the photoresist plug would not be completely covered by BaF_2. Placing the sample in acetone dissolved the photoresist and lifted-off the BaF_2 which had covered it, leaving a well defined window in the insulator.

4.7.2 Contact Metal

The top surface contact metal must make a good ohmic contact to 10^{19} n-type (PbSn)Te and must also provide sufficient lateral electrical conductivity to avoid excessive series resistance between the off-mesa wire bond and the diode itself. The metals most often used are In or Au. The nature of these electrical contacts is still the subject of theoretical discussion; at one time, In, because of its low work function, was thought to be preferable, although equally good results

have been obtained with Au, despite its high work function. Diffusion of In into n-type material is not as serious a problem as it is for p-type material since In is an n-dopant.

The metallization used for the cw lasers fabricated with chemical etching consisted of 0.1um of Indium (to provide low interface resistance) followed by 1um of copper (to provide lateral conductivity and thermal expansion match).

The metallization used for the pulsed lasers fabricated by ion-milling was 1um of Au. Au was used because it had been reported to give good contacts and because it ion-mills very readily. No underlayer of indium was used because of the tendency for In and Au to form brittle inter-metallic compounds.

Both metallization schemes (In/Cu and Au) afforded acceptable contacts. The program scope was not sufficient to complete a comparison of these contact metals. In particular, because of a very crude wire bonding technique, differences in metallization were probably obscured by other contact resistance difficulties.

Following top metal deposition, the laser is entirely covered by metal and is electrically connected to every other laser on the wafer. At this point 375um x 375um contact pads are defined by standard photolithography and wet-chemical etching (for Cu or Au) or ion-milling (for Au). The contact pad is aligned so metal is completely removed from one face of the laser, to permit output coupling. The back face remains covered with metal, automatically affording a high reflectivity. Figure 19 affords an excellent view of the rectangular diode covered by the square contact pad, while Figure 20 illustrates the square array of diodes.

4.7.3 Off-Mesa Wire Bonding

The scope of this program did not permit development of an elegant wire-bonding procedure. Gold wire, typically 50um in diameter, was fastened to the contact pad with silver-filled epoxy.

4.8 Package Completion

In the completed package, the lead wires were connected, six at a time, to a PC board. The entire package was fastened to an OFHC copper block which had clearance holes the same spacing and separation as those on the standard Laser Analytics package. Since the main thrust of the program was demonstration of reliability and performance improvement for lasers fabricated by a novel technology, no attempt was made to modify this inelegant package. Figure 21 shows a typical package. The Cu heat sink has been wire sawn, and the portion shown (roughly one fourth of the original) has approximately forty lasers on it, of which the front six have been electrically contacted. Clearly, there is room for improvement, but the advances on this package would be very straight-forward applications of well-established dicing and bonding techniques.

The most significant feature of this packaging procedure is the small mechanical stress felt by the laser itself. The (PbSn)Te is constrained on only one surface; it has one free surface. The top contact is next to the laser, not on top of it. This geometry greatly reduces the shear stresses to which the laser can be exposed and also reduces the forces felt during bonding. Finally, the laser is surrounded by material which is thermally matched to (PbSn)Te: the OFHC copper beneath it, BaF_2 insulator surrounding it, and evaporated copper above it.

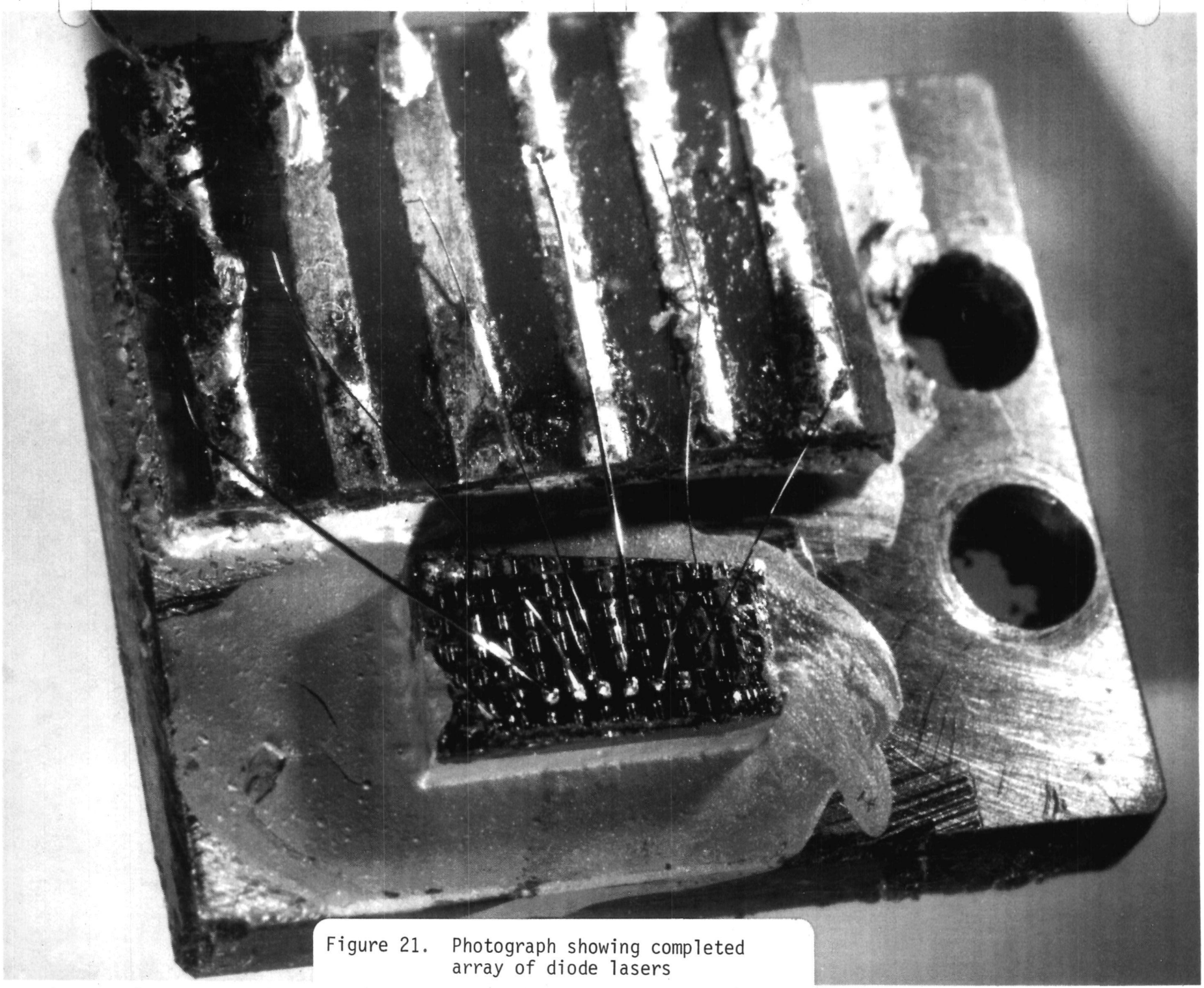

Figure 21. Photograph showing completed array of diode lasers

5.0 Device Evaluation

5.1 Electrical Measurements

5.1.1 Hall Effect

The van der Pauw technique was routinely employed to measure majority carrier concentrations and mobilities in films deposited on BaF_2 substrates, measurements were done both at room temperature and at $77^{o}K$. Growth conditions for each layer of the multilayer structures were confirmed by direct measurements of single layer films. In addition, one sample of every growth run was a 4μm thick layer of undoped (PbSn)Te which was measured to confirm the carrier concentration and mobility of the active region of the lasers. Hall measurements were used routinely for calibration, diagnosis, and monitoring the crystal growth process.

5.1.2 Capacitance - voltage

Capacitance - voltage measurements on reverse-biased p-n junctions or Schottky carriers are frequently used to measure the distribution of charge in the vicinity of the junction. It was hoped that C-V measurements could routinely be employed to monitor doping of the grown junction films, since the Hall techniques are appropriate only for homogeneous, uniform structures.

We successfully carried out C-V measurements on PbTe films, but the reverse leakage currents for the narrower band gap material (PbSn)Te prevented meaningful capacitance measurements. For PbTe, the C-V measurements implied a doping level consistent both with the target for the film and with a subsequent Hall measurement.

5.1.3 Current - voltage

Current-voltage data were routinely recorded for all diodes. However, because of our crude bonding technique, most diodes had only two-point measurements, which were dominated by the series resistance of the lead wires and the silicon-epoxy bonds. Our primary interest was to demonstrate laser action by direct optical techniques. However, periodic four-point measurements were made by

bonding two leads to one diode. Fig.22 presents four-point current-voltage data for a laser with threshold current of 0.3A indicated by the kink in the curve at that point. Lasing for all devices delivered was confirmed by optical measurements. A significant feature of the current-voltage curve is the forward series resistance of 40m Ω . For a contact area 50um x 200um, this corresponds to an RA product of 4×10^{-6} Ω -cm^2, comparable to the lowest values reported in the literature.

After lasing had been confirmed optically for a number of devices, more attention was paid to four-point series resistance measurements. In particular, since there was a highly publicized reliability problem associated with contact degradation, devices were thermally cycled and also stored at elevated temperatures. Figure 23 shows that there was no change in threshold current, threshold voltage, or forward series resistance.

Current - voltage data were also obtained for the ion-milled lasers. It was thought that ion-milling might introduce crystal damage near the junction and increase reverse leakage current. Figure 24 shows that no such effect was observed; indeed, the ion-milled lasers had lower reverse leakage than the chemically etched devices. This information is inconclusive, however, since reverse leakage for both types of structure was clearly dominated by surface currents and not by bulk generation-recombination centers or diffusion current.

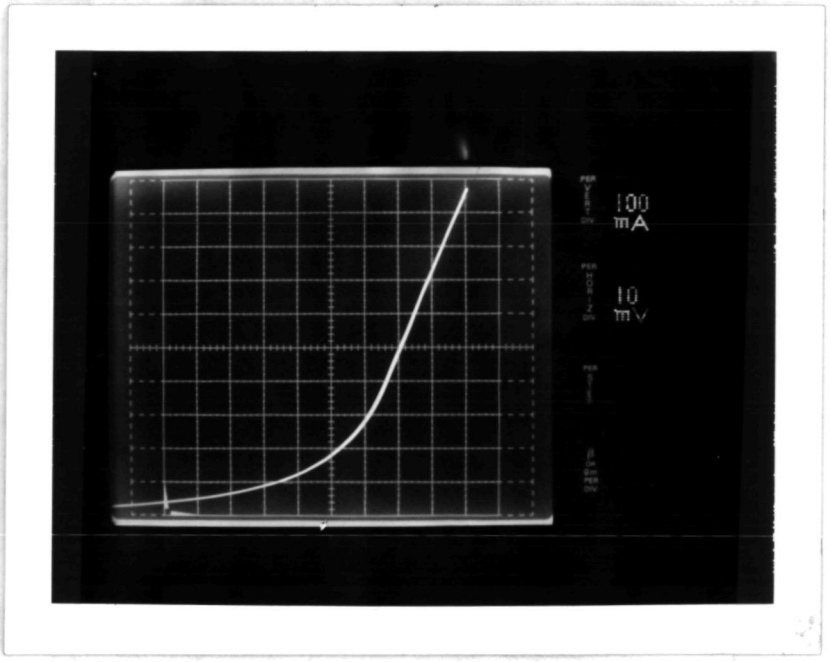

Figure 22. Current-voltage relationship for diode having threshold current of .3A at 12K. Vertical scale is .1A/division, horizontal scale (offset 50mV to the left) is 10mV/division. The kink at .3A is indicative of a lasing threshold with high internal quantum efficiency.

LIFE TEST DATA FOR P-E DIODE LASER

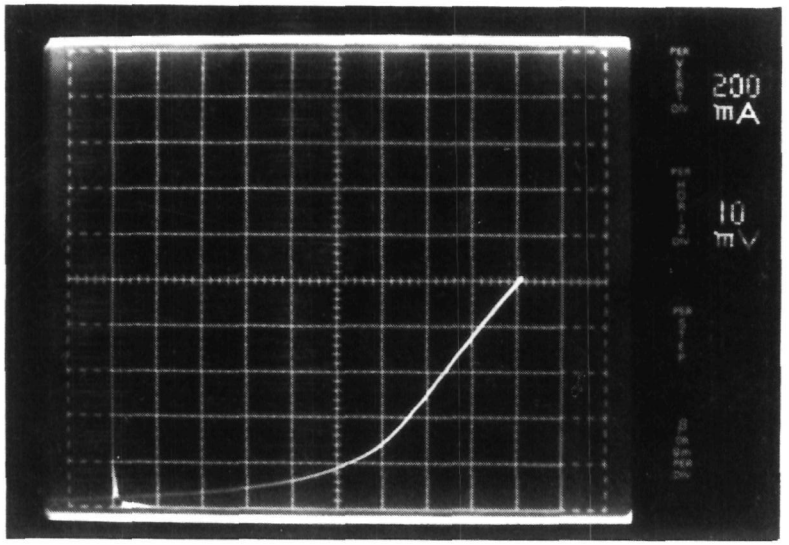

a. INITIAL CURVE

I_t = 320 mA

V_t = 112 mV

R_f = 38 mΩ

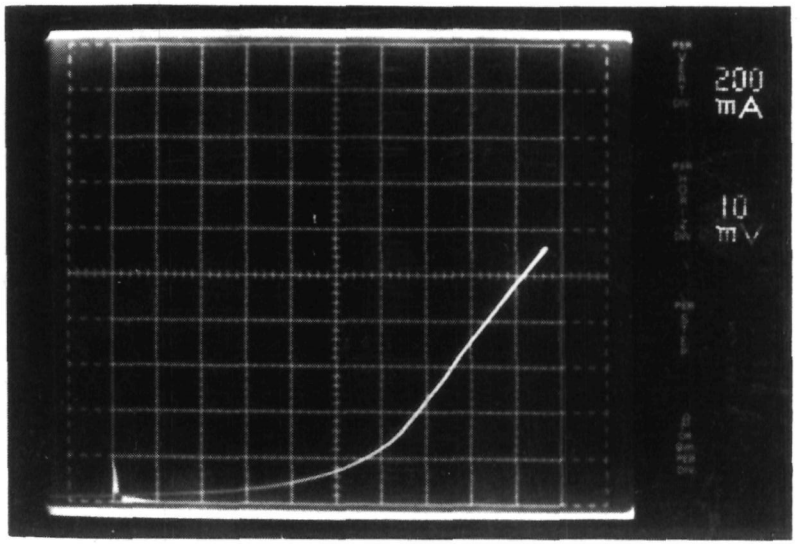

b. AFTER 10 THERMAL CYCLES TO 12°K FROM 300°K AND 4 WEEKS STORAGE AT 310°K

Figure 23. Current-voltage curves for diode laser before and after thermal cycling and storage at elevated temperature

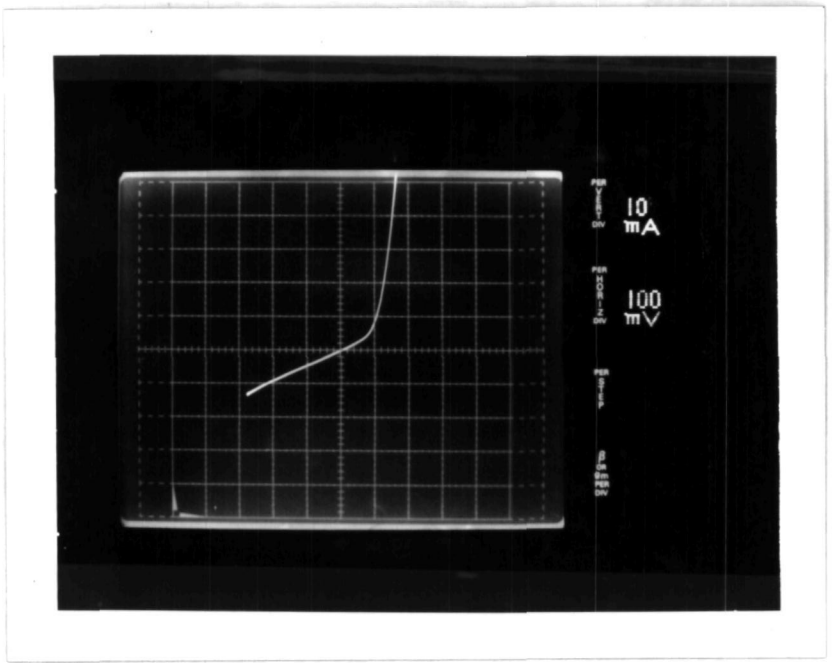

a.

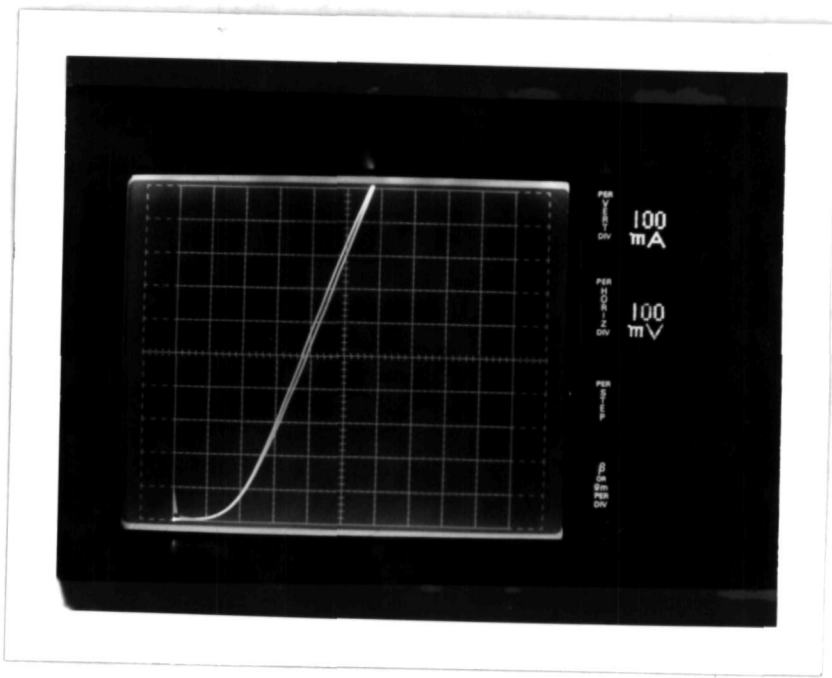

b.

Figure 24. Current voltage curves for ion-milled diode.

a. low current AC data illustrating low leakage.

b. high current forward bias data.

5.2 Optical Measurements

5.2.1 Threshold Current

Threshold current was determined from plots of light output versus current. Pulsed thresholds were determined with 5us pulses and 100 Hz repetition rate. Chemically etched devices of $(Ph_{.81}Sn_{.19})Te$ typically operated cw to temperatures of 50-60°K, while pulsed operation persisted to 95°K. Output power, even pulsed, rarely exceeded 10uw. Figures 25-28 present light-current data at several temperatures for a representative chemically etched laser, C-2, while figure 29 summarizes the pulsed threshold current as a function of temperature.

Threshold currents were not measured precisely for ion-milled lasers, however, pulsed lasing was observed at temperatures up to 45-50°K. Figure 30 illustrates the light-current curve for a representative ion-milled device. The pulsed threshold current density is approximately 10,000 A/cm^2, or ten times greater than that of a comparable chemically etched device. The threshold current remains nearly constant with increasing temperature, and figure 31 demonstrates pulsed lasing for this device (Im-7D) at 45°K. Threshold currents increased rapidly with temperature above 45°K. These devices did not operate cw, and suffered from abnormally high contact resistance. However, unlike chemically etched devices (with sloping sidewalls) the ion milled devices showed no saturation in output power until excessive contact heating catastrophically destroyed the devices. Figure 32 shows the pulsed output for a device driven with 3.5A at 12°K. Allowing for poor optical coupling from the device to the detector, the estimated output power is 30-50uw.

Continuous wave thresholds were determined from scans of spectral output as a function of current and temperature. Threshold current densities at low temperatures were comparable to pulsed thresholds. However, the maximum current which the devices could stand was only about 10000A/cm^2 (cw). Junction heating was a serious problem, and was the most serious restriction on cw operating range.

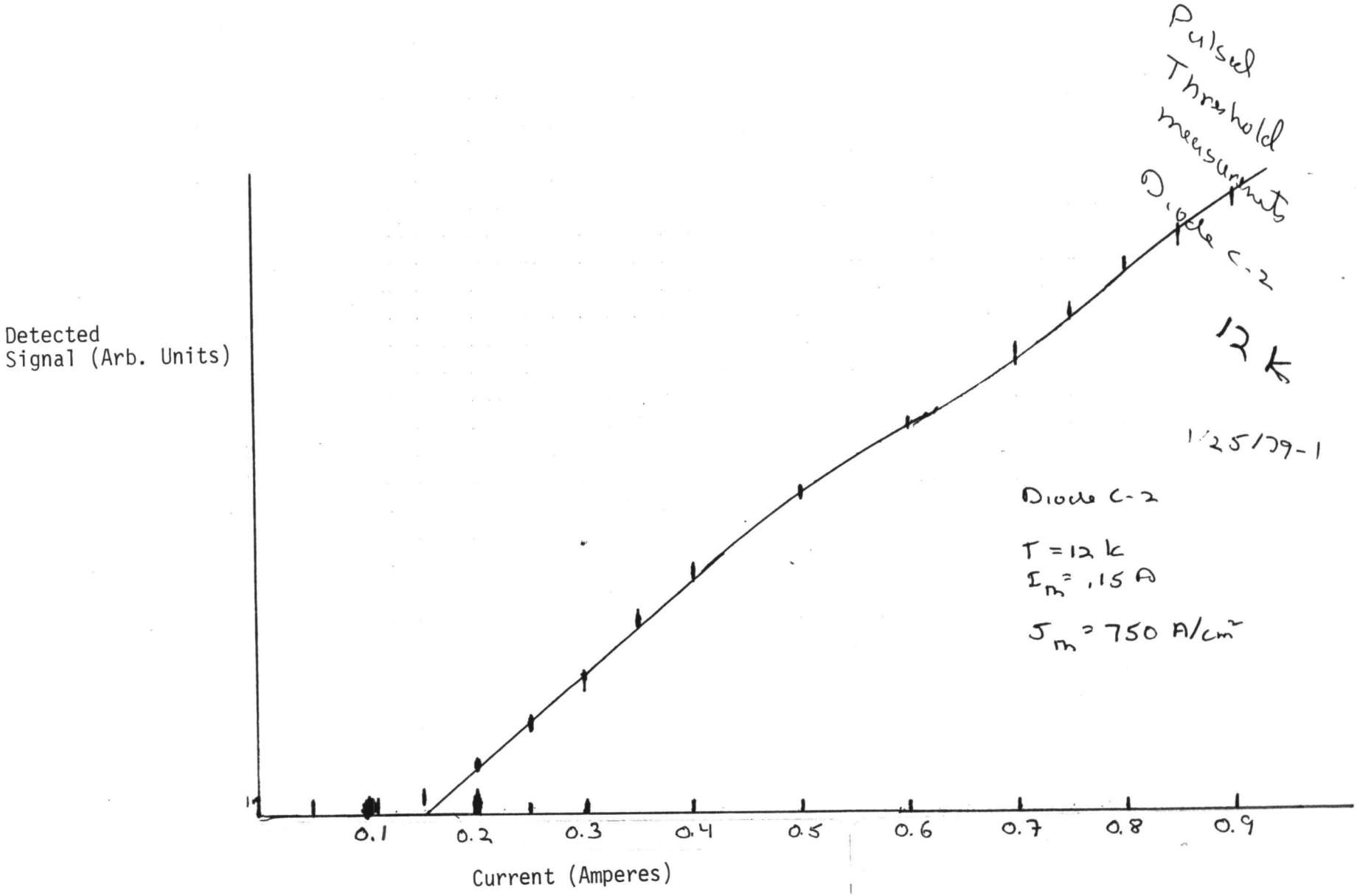

Figure 25. Detected signal vs current for 5μs pulses at 100 Hz repetition rate. Data for diode c-2 at 12°K

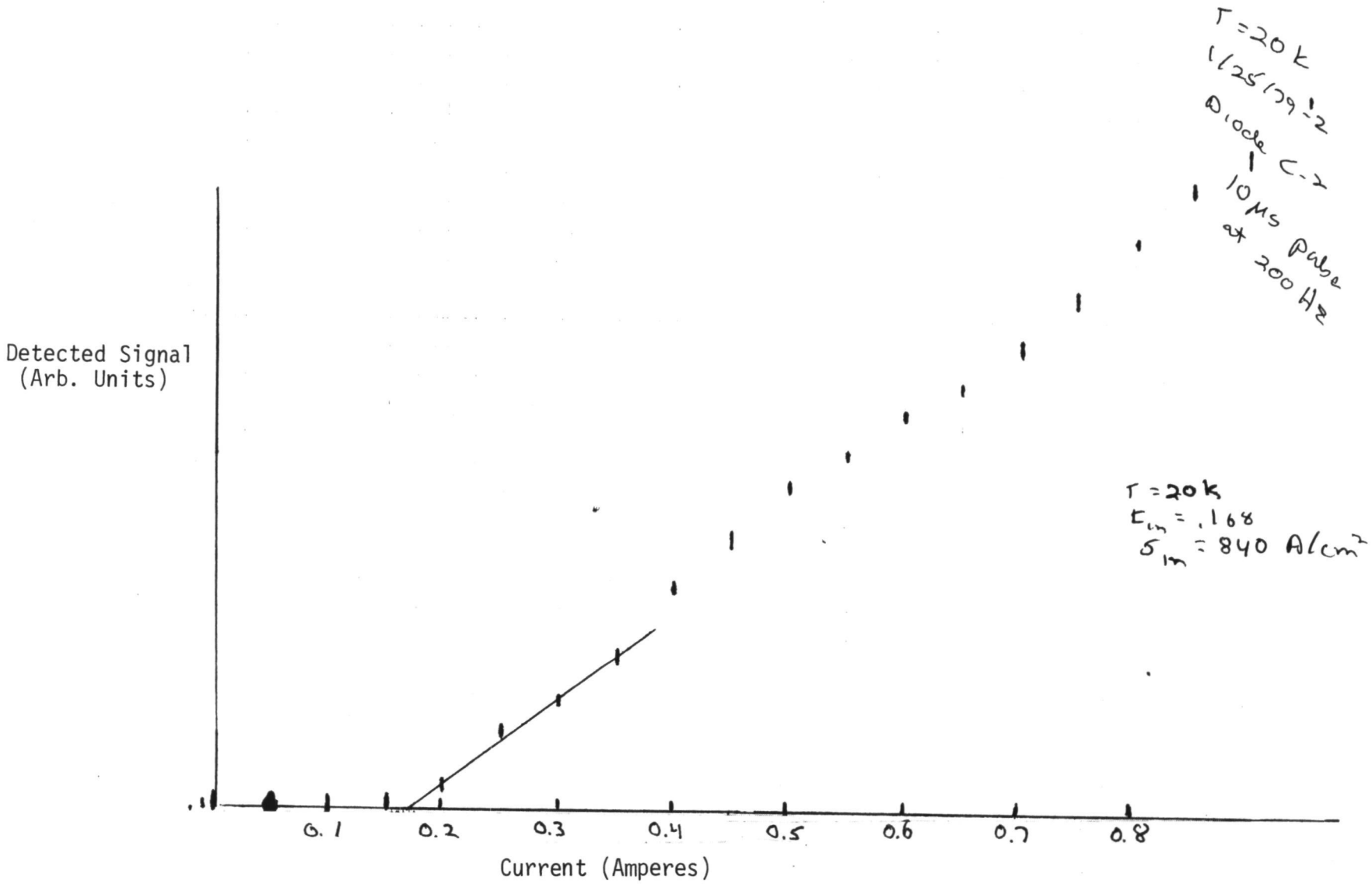

Figure 26. Detected signal vs pulsed current at 20°K

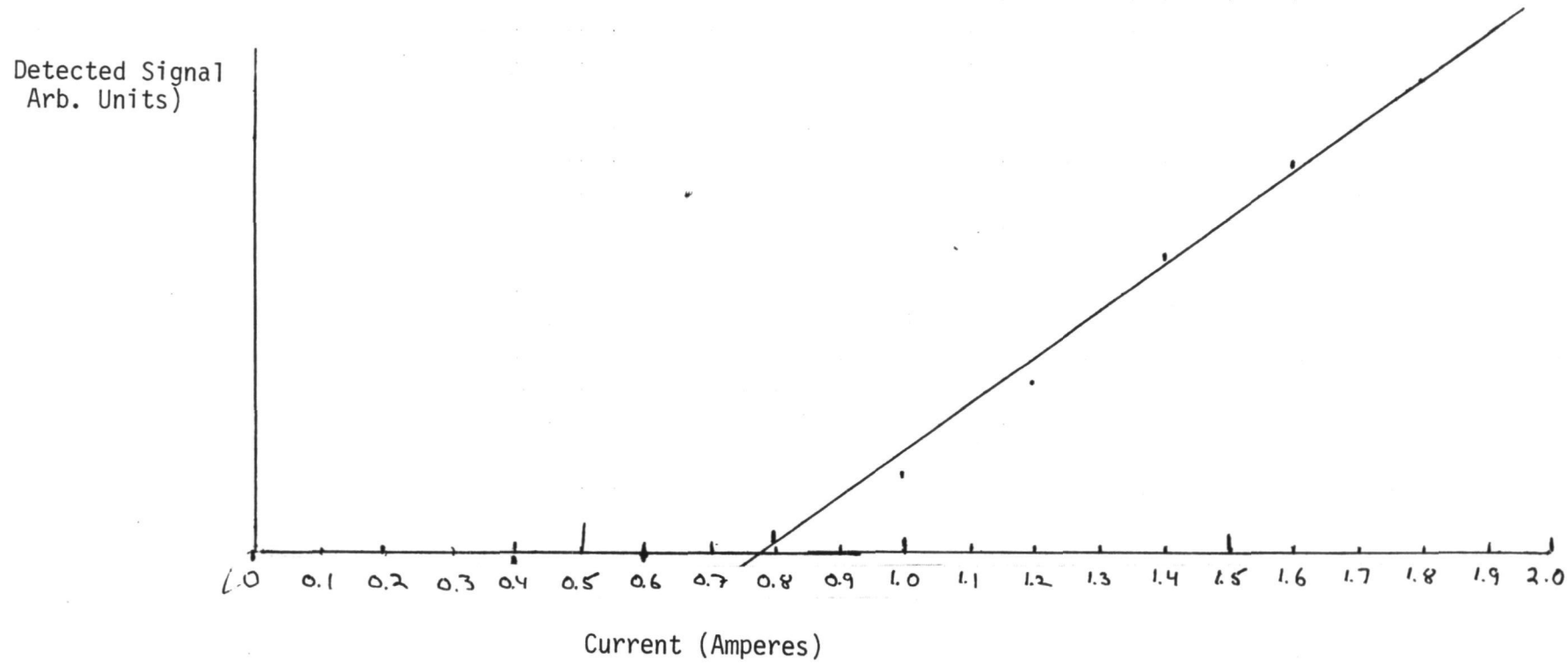

Figure 27. Detected signal vs pulsed current at 75°K

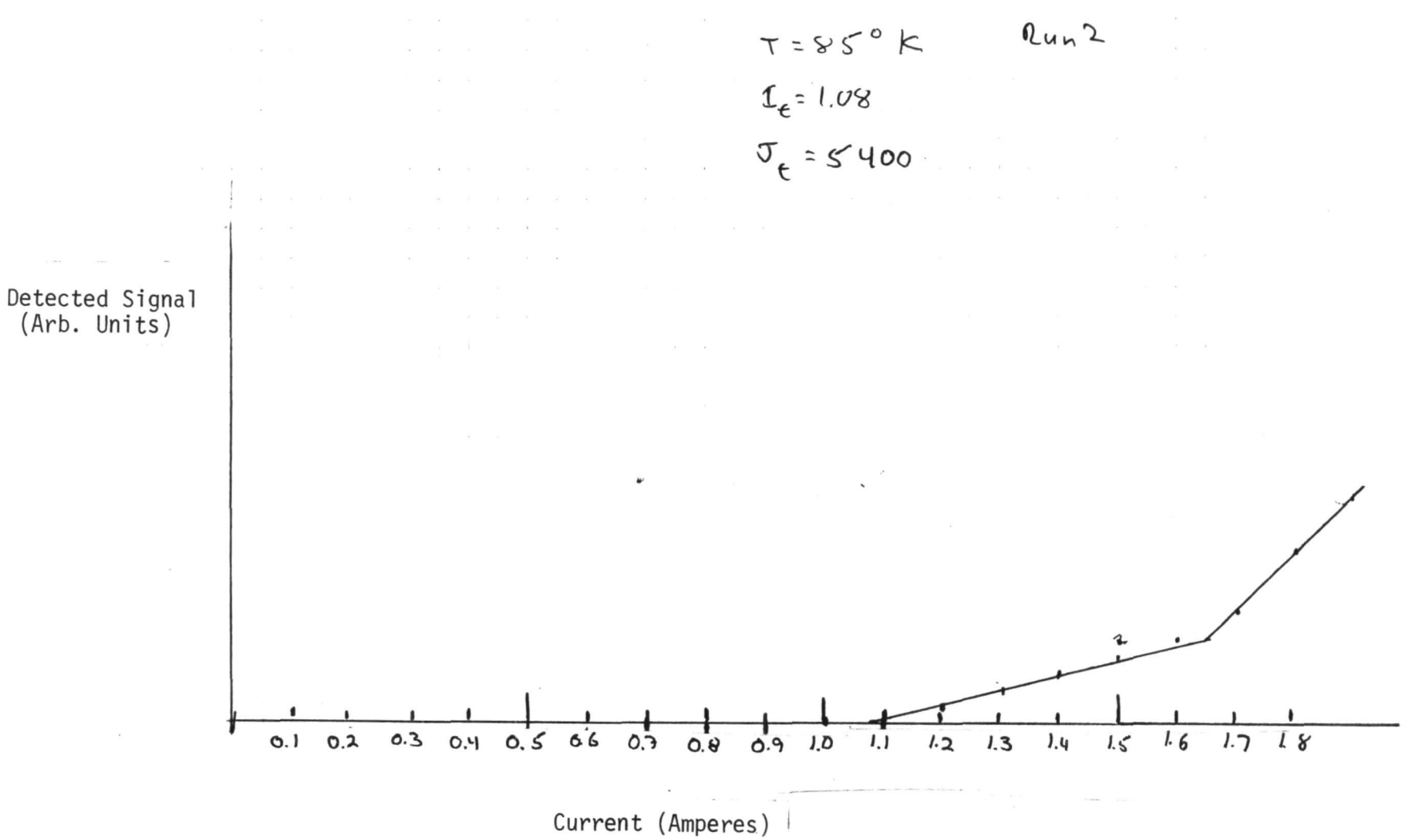

Figure 28. Detected signal vs pulsed current at 85°K

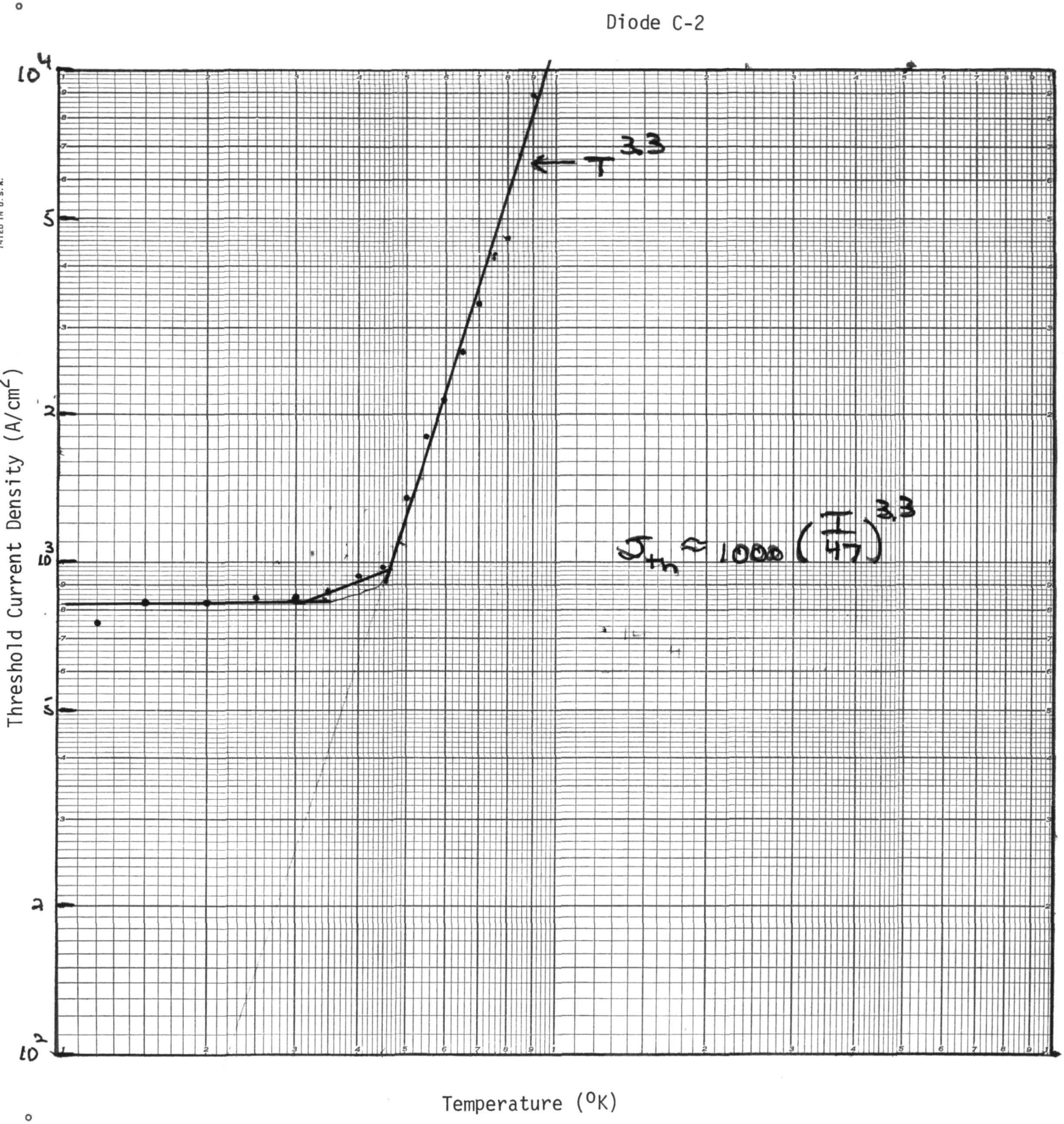

Figure 29. Temperature dependence of pulsed threshold current

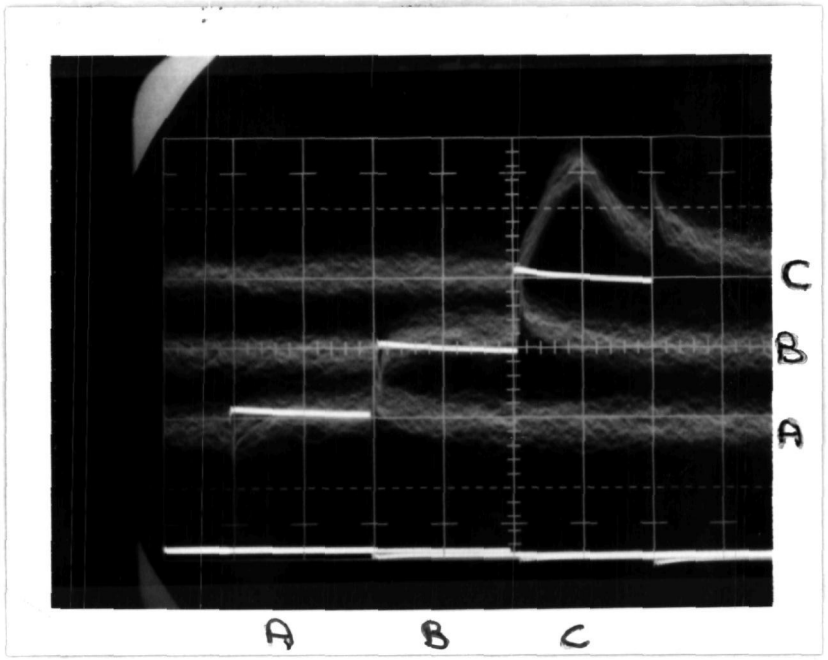

Figure 30. Pulsed light output as a function of pulsed current at 12°K. 5μs/div, .5 A/div. Solid lines are current in diode.

A. I = 1 amp
B. I = 1.5 amp
C. I = 2.0 amp

I_t is between 1.5 and 2.0 amp.

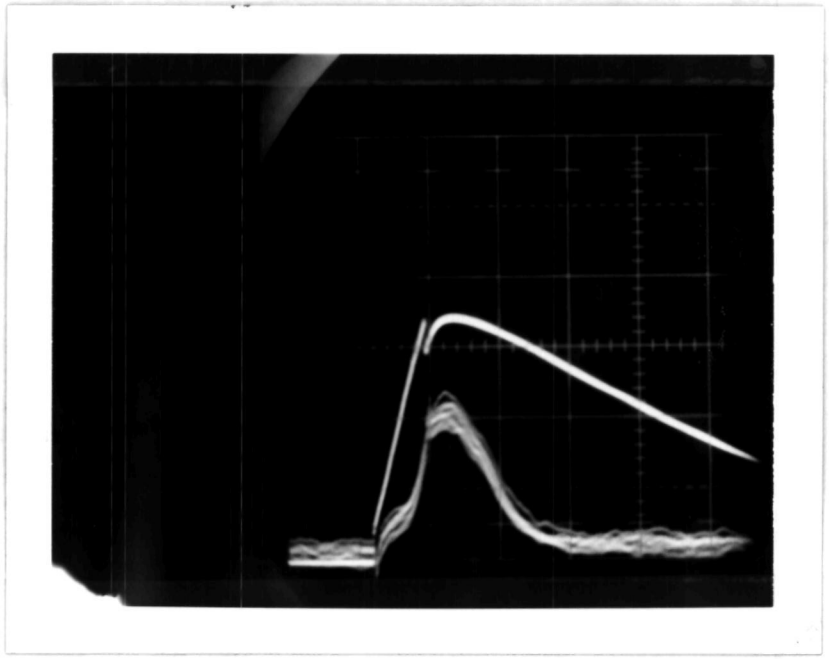

Figure 31. Pulsed light output at 45°K. Solid line is current at 1 amp/div, horizontal scale is 5μs/div.

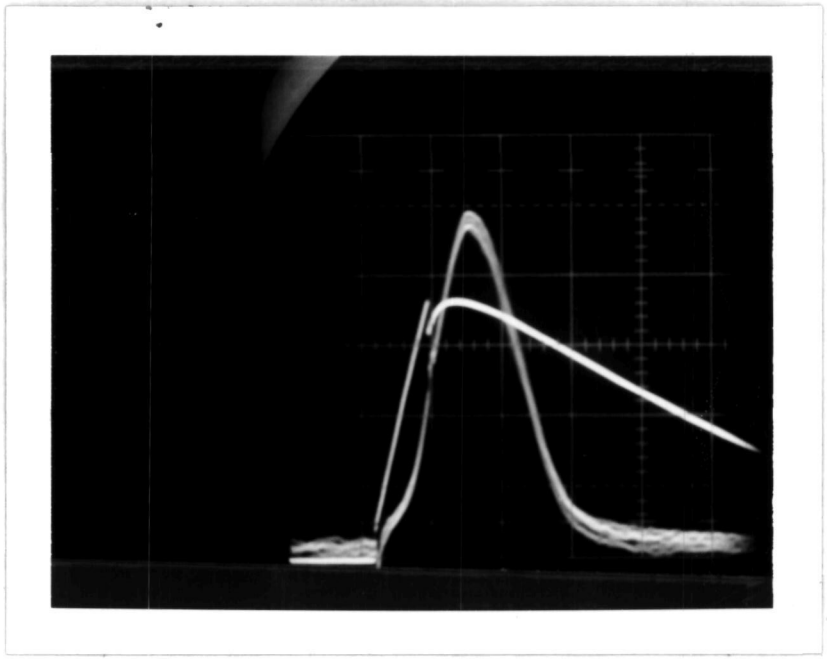

Figure 32. Pulsed light output at 12°K. Total pulsed power received at the detector is about 10μw. Solid line is current pulse at 1 amp/div, horizontal scale is 5μs/div.

5.2.2 Spectral Properties

Output spectra were measured as a function of current and heat sink temperature for cw operation. Measurements were also made for pulsed operation, but these spectra were very difficult to interpret because of chirping (wavelength tuning as the diode heated up) during the pulse.

Figures 33-37 are output spectra obtained from chemically etched laser C-2 for a heat sink temperature of $15^{o}K$. The onset of lasing was at a current of 0.25A (1300 A/cm^2) and lasing persisted to 1.35A. At 1.4A, lasing was quenched by excessive heating. The laser's cw tuning range was from about $760cm^{-1}$ to 990 cm^{-1}. Similar spectra were obtained as a function of heat sink temperature, until a temperature was reached, typically 50-$60^{o}K$, for which no cw spectra could be obtained. The behavior of all lasers tested was reproducible in terms of coarse wavelengths and operating temperatures and current. Specific details of mode structure varied greatly from device to device. The typical operating range is summarized in figure 38 where the average wavelength (the center frequency for multimode emission) is plotted as a function of heat sink temperature and current. The temperature rise at the junction can be estimated by comparing cw output spectra to pulsed spectra, and using equation (1) to estimate the bandgap as a function of temperature. The result obtained is quite insensitive to the estimated value of X, the mole fraction of SnTe. The solid lines were computed from X = 0.18, using the measured I-V data to estimate power input to the device. For this "typical" device, the pulsed output wavelength at $95^{o}K$ was about 10μm, consistent with the prediction based upon equation 1 and X = 0.18. One inescapable conclusion is that there was considerable room for improvement in heat sinking; at a heat sink temperature of $15^{o}K$ and a current of 1.35A (7200 A/cm^2) the junction temperature was $95^{o}K$, a temperature rise of $80^{o}K$. A more typical value for a well heat-sunk device would be about $20^{o}K$. An equivalent

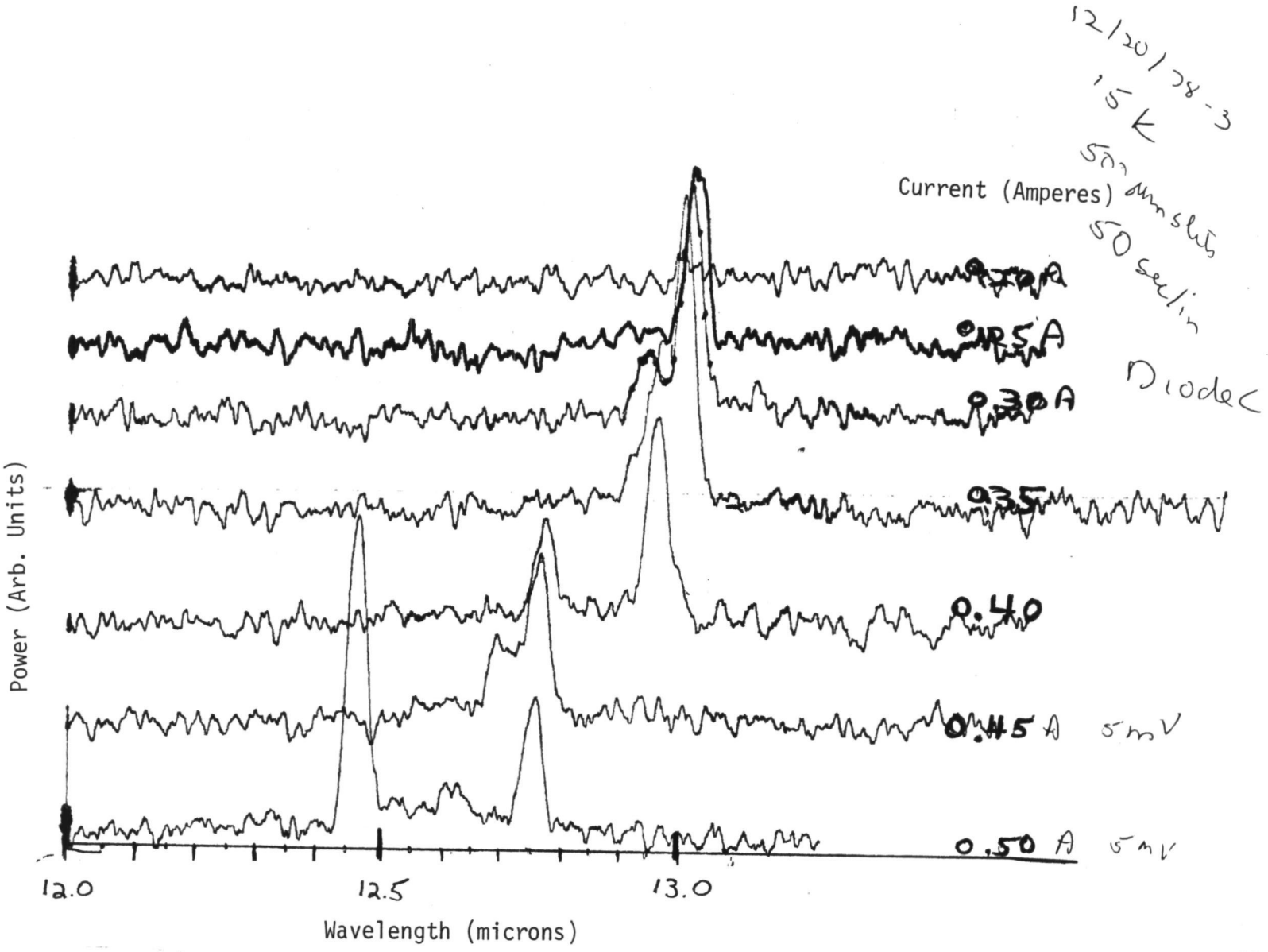

Figure 33. CW output wavelengths (microns) at 15°K as a function of current from 0.25A to 0.5A.

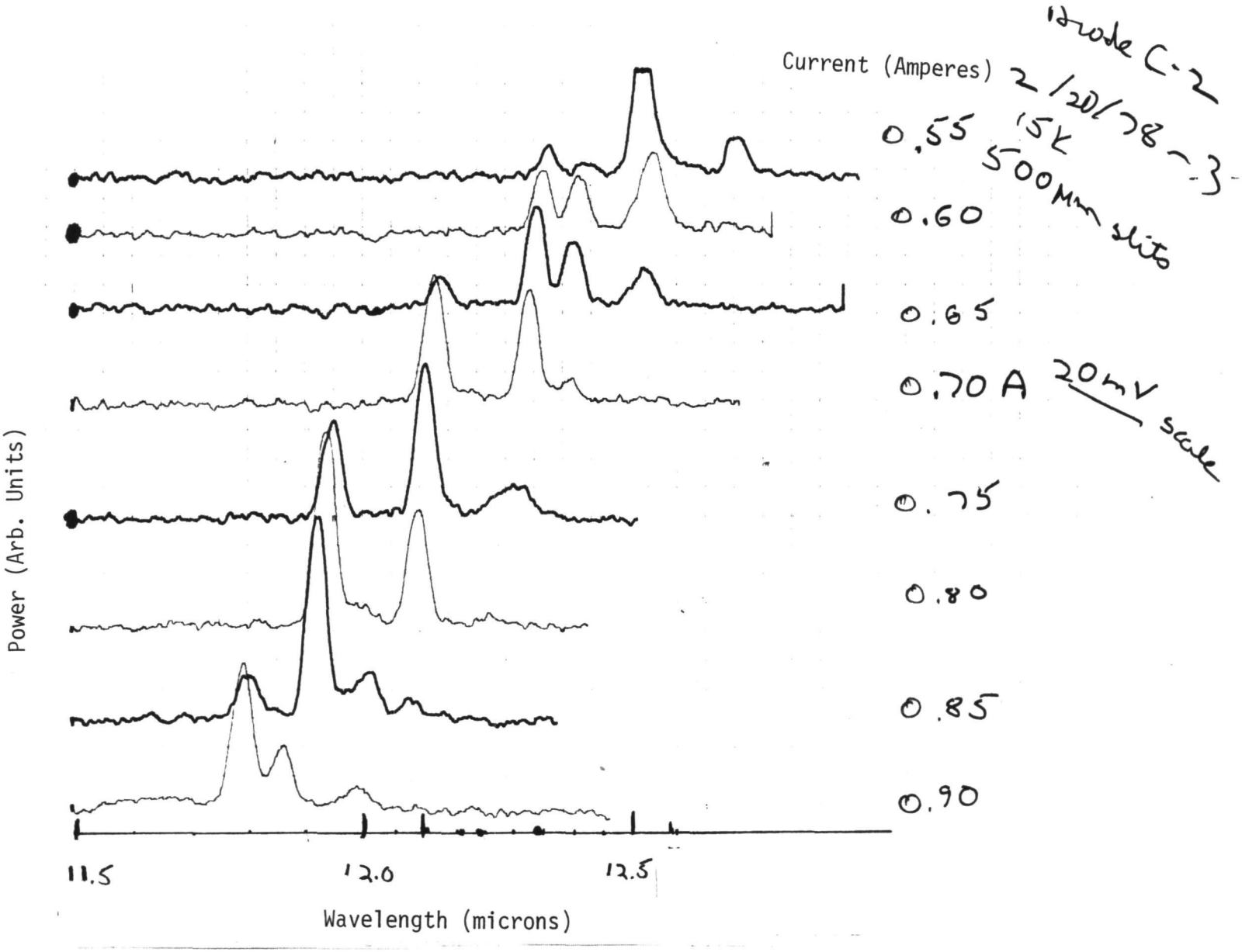

Figure 34. CW output wavelengths at 15°K for currents from 0.55A to 0.90A.

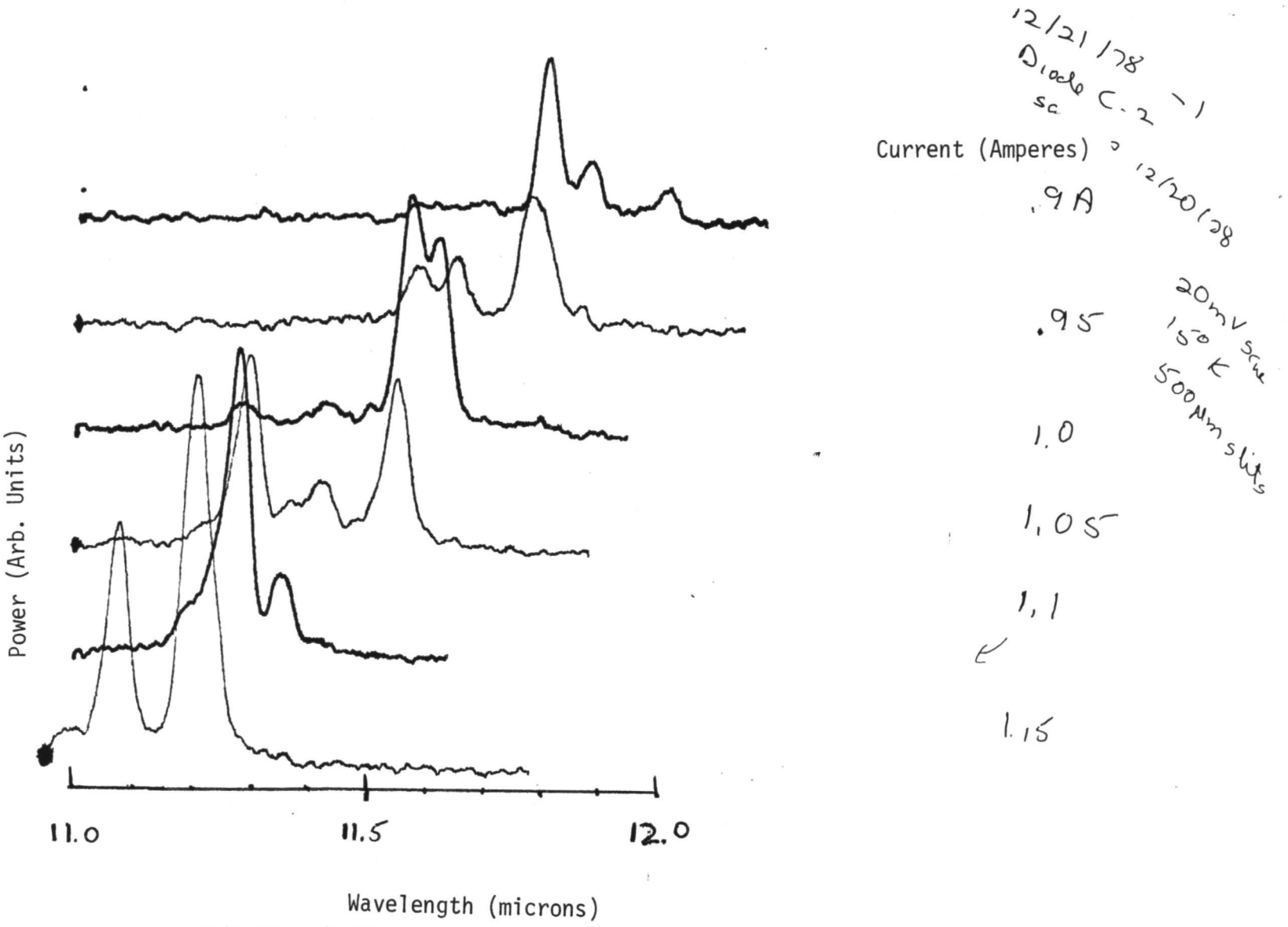

Figure 35. CW output wavelengths at 15°K for currents from 0.90A to 1.15A.

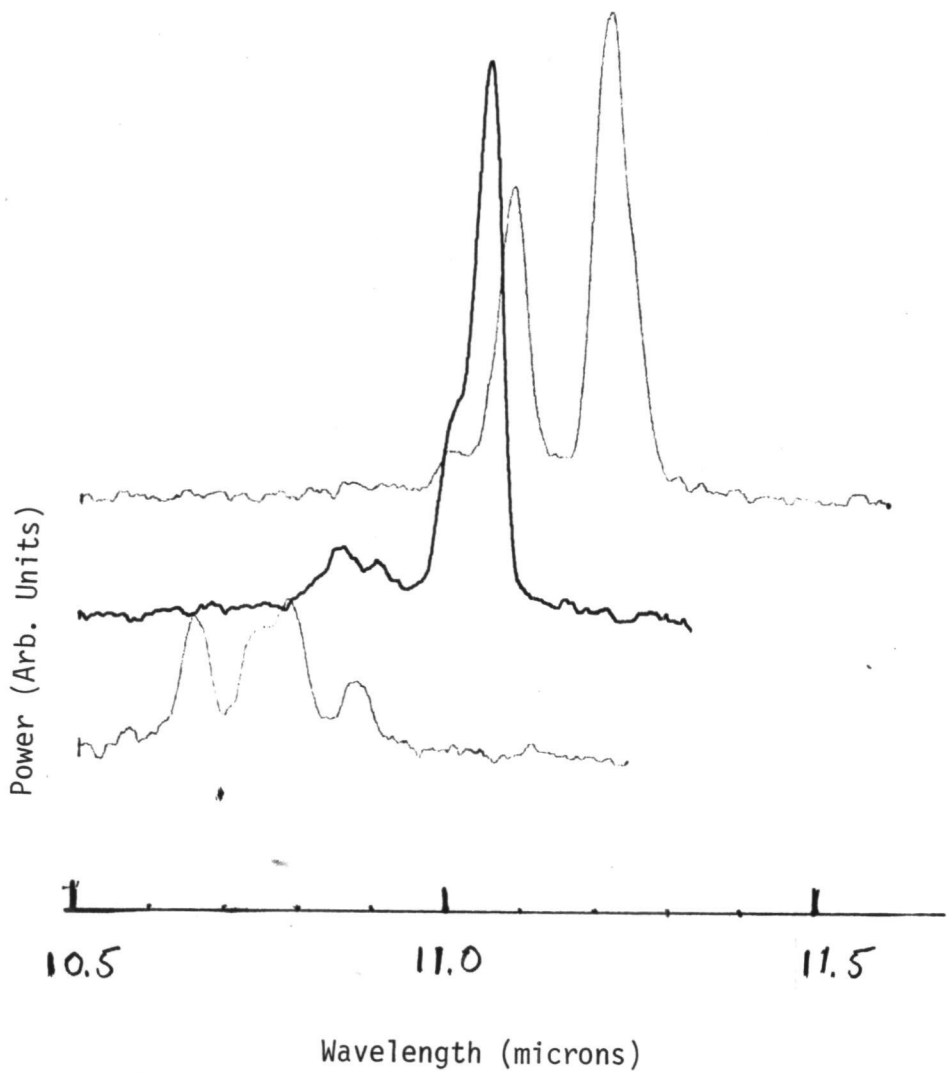

Figure 36. CW output wavelength at 15°K for currents from 1.15A to 1.25A.

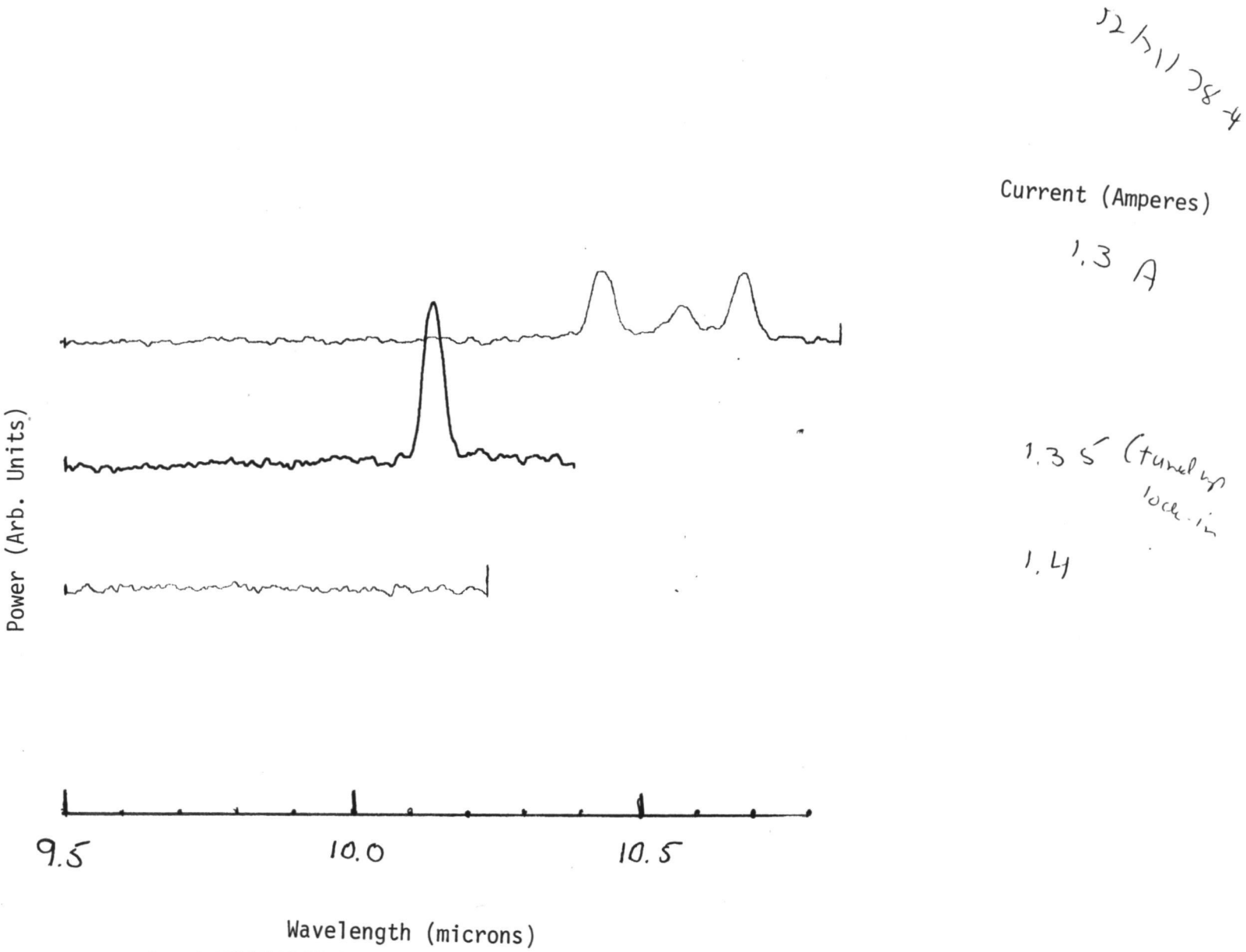

Figure 37. CW output wavelength at 15°K for currents from 1.3A until lasing ceased at 1.4A.

OPERATING RANGE OF TYPICAL DIODE LASER

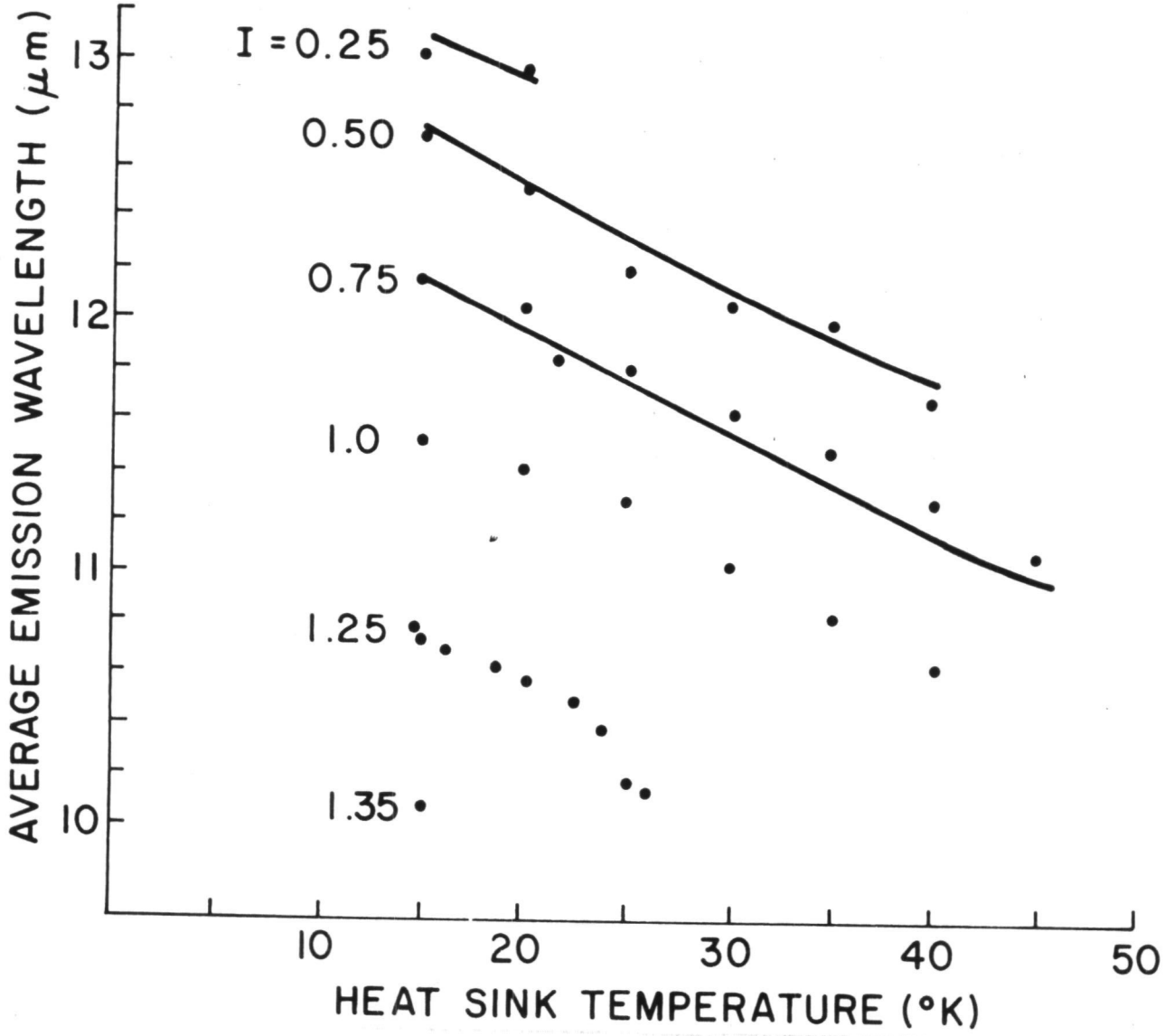

Figure 38. Continuous wave emission wavelength as a function of temperature for currents from 0.25 to 1.35A

way of stating this result is that if the devices had a junction temperature rise of only $20^{o}K$, they would have operated cw up to $75^{o}K$. A similar line of reasoning suggests that the ion-milled devices, which operated pulsed up to $45^{o}K$, would have operated cw with better heat sinking.

5.2.3 Output Power

Despite their wide tuning range, relatively low threshold currents, and capability of operation at elevated temperature, the lasers fabricated for this program had very little output power. The chemically etched devices, operating pulsed or cw, would typically saturate at about 10 uw received power on the detector.

The ion-milled structures showed no such saturation effect, lending some credence to the theory that the earlier devices were adversely affected by sloping sidewalls on the Fabry-Perot cavities. However, the ion-milled structures had such high series resistance that cw operation was not possible. They also showed quite low, albeit not saturated, pulsed output power; an optimistic estimate would be 50 uw multimode at 3A (80,000 A/cm^2).

6.0 Reliability

Reliability of Pb-salt lasers have been a subject of considerable controversy. At the outset of this program, lasers were reputedly plagued by two problems: room temperature shelf life and degradation from thermal cycling. Both failure modes were manifested by excessive series resistance in the diodes.

The approach taken in this program was to design devices which would not be subject to these particular modes of failure. The thermal cycling problem was quite clearly related to the packaging. The die bonding scheme used in this program specifically addressed the problem of shear during thermal cycling. The room temperature shelf life problem was felt to be related to indium diffusion. Great care was taken in formulating a metallization method which specifically prevented indium from diffusing into the p-type semiconductor. As a result, as illustrated by figure 23, the devices fabricated in this program proved the existence of reliable packaging and metallization. Devices were stored at room temperature for over 18 months and showed no degradation, and no degradation was observed as a result of thermal cycling.

REFERENCES

1) W.W. Anderson, "Gain-Frequency-Current Relation for $Pb_{1-x}Sn_xTe$ Double Heterostructure Lasers", IEEE Journal of Quantum Electronics QE-13, 532 (1977).

2) D.L. Smith and V.Y. Pickhardt, "Impurity Dopant Incorporation and Diffusion During Molecular Beam Epitaxial Growth of IV-VI Semiconductors", J. Electrochem Society 125, 2042 (1978).

3) D.L. Smith, D.P. Mathur, and V.Y. Pickhardt, "High Performance (PbSn)Te Detectors by Molecular Beam Epitaxy", presented at IRIS Detector Specialty Group Meeting, Ft. Monmouth, N.J. (March 1975).

4) W.H. Weber and K.F. Yeung, "Waveguide and luminescent properties of thin-film Pb-salt injection lasers", Journal of Applied Physics 44, 4991 (1973).

5) A.R. Calawa, T.C. Harman, M. Finn, and P. Youtz, Trans. Metall. Soc. AIME 242, 375 (1968).

6) P.M. Asback, M.I.T. Ph.D. Thesis, 1975.

7) J.N. Walpole, S.H. Groves, and T.C. Harman, "MBE Homostructure PbTe Diode Lasers with CW Operation up to 100K", Device Research Conference, June 27-29, 1977, Ithaca, N.Y.

8) Wayne Lo, "Homojunction Lead-Tin-Tellunide Diode Lasers with Increased Frequency Tuning Range", IEEE Journal of Quantum Electronics QE-13, 591 (1977).

1. Report No.	2. Government Accession No.	3. Recipient's Catalog No.
NASA CR-165683		

4. Title and Subtitle	5. Report Date
DEVELOPMENT OF MBE GROWN Pb-SALT SEMICONDUCTOR LASERS FOR THE 8.0 TO 15.0 MICROMETER SPECTRAL REGION	March 1981
	6. Performing Organization Code

7. Author(s)	8. Performing Organization Report No.
Matthew D. Miller	15194
	10. Work Unit No.

9. Performing Organization Name and Address	11. Contract or Grant No.
Perkin-Elmer Corporation 100 Wooster Heights Road Danbury, CT 06810	NAS1-14996
	13. Type of Report and Period Covered Contractor report

12. Sponsoring Agency Name and Address	14. Sponsoring Agency Code
National Aeronautics and Space Administration Langley Research Center Hampton, Virginia 23665	

15. Supplementary Notes

Langley technical monitor: Dr. James Hoell
Final Report

16. Abstract

Diode lasers were fabricated using multiple source molecular beam epitaxial growth of (PbSn)Te on BaF_2 substrates. Methods for crystal growth, crystal transfer, and device fabrication by photolithographic techniques were developed. Lasers operated in the spectral range from 10μm to 14μm and at temperatures from 12°K to 60°K continuous wave and to 95°K pulsed.

17. Key Words (Suggested by Author(s))	18. Distribution Statement
	Unclassified Unlimited

19. Security Classif. (of this report)	20. Security Classif. (of this page)	21. No. of Pages	22. Price*
Unclassified	Unclassified		

For sale by the National Technical Information Service, Springfield, Virginia 22161